Chapter 5
Digital Signal Processing of Experimental Pressure Signal

Abbreviations and Symbols

BDC	Bottom dead center
bTDC	Before top dead center
CA	Crank angle
CI	Compression ignition
COV	Coefficient of variation
CR	Compression ratio
CRR	Combustion reaction rate
DFT	Discrete Fourier transform
FIR	Finite impulse response
HCCI	Homogeneous charge compression ignition
IDI	Indirect injection
IIR	Infinite impulse response
IMEP	Indicated mean effective pressure
LPA	Least-square polynomial approximation
LSM	Least-square method
PSD	Power spectral density
SI	Spark ignition
TDC	Top dead center
VFO	Variable frequency oscillator
E_{bias}	Sensor offset voltage
K_{S}	Sensor gain
k	Harmonics
n	Polytrophic exponent
P	Pressure
P_{cyl}	True cylinder pressure
P_{offset}	Pressure offset
P_{peg}	Absolute pressure value at the pegging position

R. K. Maurya, *Reciprocating Engine Combustion Diagnostics*, Mechanical Engineering Series, https://doi.org/10.1007/978-3-030-11954-6_5

ΔP	Pressure difference
$p(\theta_{\text{ref}})$	Cylinder pressure at a reference crank angle
V	Volume
$V(\theta_{\text{ref}})$	Cylinder volume at a reference crank angle
θ	Crank angle position
θ_{peg}	Crank angle position of pegging point
τ	Normalized time
ξ	Combustion reaction rate
σ	Standard deviation

5.1 Introduction

In-cylinder pressure measurement and analysis is the key tool for engine research and diagnosis since the advent of the reciprocating engine. In-cylinder pressure signal provides a large amount of information that can be used for analyzing combustion process and combustion quality. The accuracy of pressure measurements governs the quality of analysis of engine combustion process. In the last two decades, the real-time engine control and onboard supervision based on pressure signal have also become of particular interest to the automotive industry. Thus, measurement of the undistorted and unbiased cylinder pressure signal is essential for cylinder pressure-based combustion analysis and control. In-cylinder pressure is typically measured by piezoelectric transducer installed on the engine head (see Chap. 2). The experimental pressure signal typically requires four-step data processing before extracting the valuable information regarding the engine combustion process [1]. Four-step experimental signal data processing includes (1) crank angle phasing, (2) absolute pressure referencing, (3) cycle averaging, and (4) filtering (smoothening) [1, 2]. In-cylinder pressure data obtained from signal processing is used for further analysis to get information about engine combustion characteristics. The piezoelectric pressure transducer is based on the concept that measures only the variation in the combustion chamber pressure rather than the pressure itself. Hence, absolute pressure referencing (pegging) of the signal form piezoelectric transducer is required to get the absolute values of cylinder pressure. Different methods of pegging the pressure signal are discussed in Sect. 5.3. To perform an accurate combustion and performance analysis, a precise angle phasing between pressure and piston position (cylinder volume) is essential. The measured cylinder pressure is a function of piston position (cylinder volume), and thus, determination of exact crank angle for each pressure sample is of vital importance. Section 5.2 provides the various methods for crank angle phasing (TDC phasing) of experimental cylinder pressure signal. There exist various sources of error that affect the measured pressure signal even with the good performance of the piezoelectric sensor. Typical sources of error in measured pressure data include inaccurate calibration of the cylinder pressure measurement system, signal drift due to thermal shock, mechanical vibration noise and electrical noise along with the error in pressure referencing, and crank

angle phasing [1]. The extent of error in combustion analysis by each of these sources of errors depends on the type of analysis to be conducted. The combustion parameters are typically calculated from the estimated heat release rate from measured cylinder pressure data. The heat release computation is typically affected by all these errors to some extent. Different averaging and filtering methods (Sects. 5.4 and 5.5) are used for minimizing some of the errors. Four-step digital signal processing is traditionally applied offline in such a way that allows a long signal processing time [3]. Recent developments in engine technologies demand advanced real-time diagnosis and control strategies, where long signal processing time cannot be affordable. Therefore, real-time signal processing methods with less processing time is required for engine control. The signal processing methods for offline as well as real-time application are discussed in the present chapter.

5.2 Crank Angle Phasing of Pressure Signal

Inaccurate determination of TDC, leading to the incorrect phasing of crank degree and measured cylinder pressure, is one of the most common errors that need to be eliminated for accurate calculation of combustion parameters. Incremental crank angle encoders are typically used for combustion pressure measurement. Encoders generate two signals in which one for crank angle mark (crankshaft position) and the other of one pulse per rotation for trigger signal. The trigger is used to determine the absolute position of the crankshaft. During the installation of crank angle encoder, the accurate determination of trigger mark relative to the true crank position is not always possible. Hence, a method is required to measure and establish the position of the trigger mark correctly with respect to the absolute position of the crankshaft, which is typically known as TDC determination [4]. After the determination of TDC offset, the measured crank angle marks can be shifted by the combustion measurement system to determine absolute crank position. Ideally, the peak pressure position should be at TDC position (minimum volume) during motoring conditions. However, in actual (real) motoring condition of the engine, the peak pressure precedes the TDC position due to wall heat transfer and mass losses. Figure 5.1 illustrates the TDC phase lag error with respect to motoring cylinder pressure. The difference between actual TDC position and the crank position corresponding to peak motoring pressure is defined as thermodynamic loss angle (Fig. 5.1). The TDC phase lag error ($\Delta\phi$) is defined as the angle between the peak pressure with the actual TDC and the peak pressure with a wrong TDC [5]. The thermodynamic loss angle creates the main difficulty in establishing the absolute position of the crankshaft using cylinder pressure measurement.

Determination of the absolute crankshaft position is imperative to the accuracy of subsequently calculated combustion analysis parameters. The slightest error in the measurement of crankshaft position is typically magnified by at least an order of magnitude with respect to calculations such as IMEP. Crankshaft position must be estimated accurately with respect to TDC position within 0.1° for calculation of

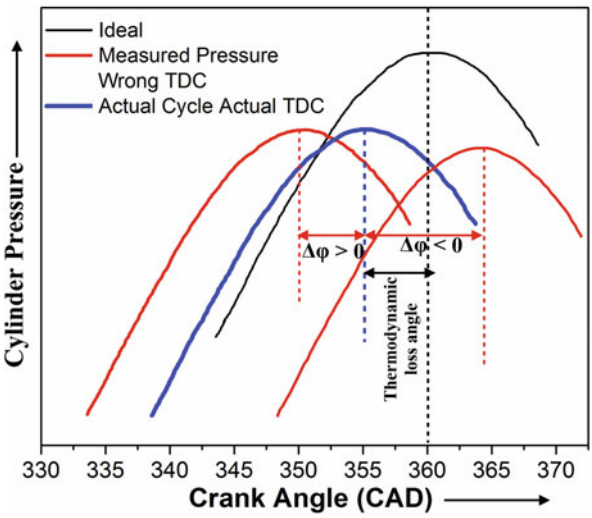

Fig. 5.1 Illustration of TDC phase lag error with respect to motoring cylinder pressure (Adapted from [5])

combustion parameters with sufficient accuracy [4]. The TDC offset determination methods can be categorized mainly into two groups based on hardware requirements for measurement [6]. The first group of methods requires additional hardware for measurement to determine the accurate TDC position, and these methods include dial gauge method (static determination), capacitive probes, microwave, etc. The second group of methods do not require additional hardware but use in-cylinder pressure signal, which is any way installed for combustion measurement. These methods are based on algorithms which determines the TDC position from measured in-cylinder pressure as a function of the crankshaft position. Various methods for determination of TDC position for crank angle phasing are discussed in the following subsections.

5.2.1 Phasing Methods Using Additional Hardware

5.2.1.1 Static TDC Determination

The TDC position can be determined both statically (with a dial gauge) and dynamically. In the static TDC determination method, measurement of TDC position is taken at the stationary crankshaft. Mechanical and manual intervention at the engine is involved in this method. The static TDC position is determined using the measurement of piston displacement. The engine flywheel or pulley can be marked to show the correct TDC position [4]. Figure 5.2 schematically illustrates the static TDC determination method. In this method, access to the piston with a dial gauge precision measurement device is required as additional hardware. The dial gauge can be installed through spark plug or fuel injection bore for the measurement of piston

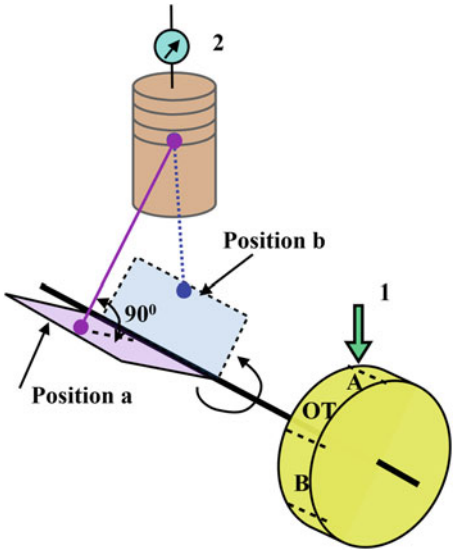

Fig. 5.2 Illustration of static TDC determination method (Courtesy AVL)

height. The crankshaft is rotated around 90° after TDC, and the depth of piston with dial gauge reading is recorded. Additionally, the pulley or flywheel is also are marked. The crankshaft is then further rotated manually with the effect of slowly lowering and then raising the piston until the exact same reading is obtained on the dial gauge. The pulley or engine flywheel is marked again relative to the static mark. Now, there are two marks on the flywheel, and two marks are exactly at the same distance from TDC. Thus, center of position between these two marks is the precise static TDC position.

In the static determination of TDC position, it is necessary to choose the position of marking on flywheel at an angle with sufficient distance from TDC. The reason for selecting the sufficient distance from TDC position is that piston movement around TDC is very small per degree of crankshaft movement [4]. However, the actual angle at which measurement is taken depends on the reach of the measuring equipment and the availability of access to the piston crown. The statically determined TDC position differs from the TDC that prevails during engine operation (i.e., dynamic TDC) due to the nonideal rigidness of the mechanical structure of reciprocating engines. Therefore, dynamic TDC determination methods are to be preferred [7].

5.2.1.2 Capacitive Probes (TDC Sensor)

The real dynamic TDC position can be determined using the TDC sensor with high levels of accuracy. In this method, the TDC sensor directly measures the piston displacement and can accommodate the elasticity of the crankshaft. This dynamic TDC determination method required additional hardware (capacitive probe), and it

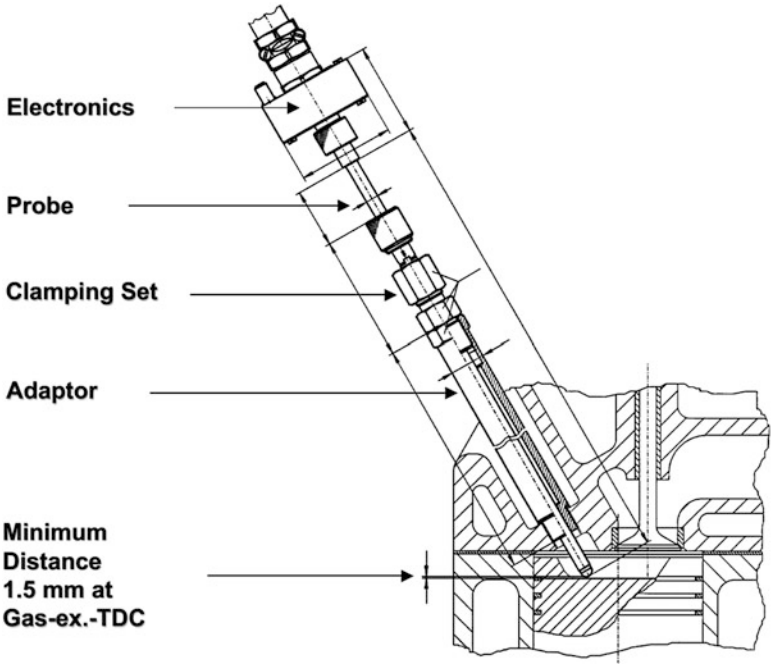

Fig. 5.3 Assembly and mounting of TDC sensor (Courtesy AVL)

can estimate the TDC position to an accuracy of 0.1° of crank angle [4]. The access of TDC sensor to the combustion chamber can be provided with an existing bore such as spark plug, glow plug, or fuel injector. Figure 5.3 presents the typical assembly and mounting of the TDC sensor on the engine head. The major components of the TDC sensor typically include the actual sensor, clamping piece, the adaptor, and evaluation electronics. The direct determination of TDC is beneficial in comparison to motoring cylinder pressure-based methods because this method does not require any correction by computing the degree of the thermodynamic loss angle. Additionally, no special machining or preparation of the engine is required, and thus, TDC sensor can be installed in a reasonably short time with high accuracy.

The functional principle of the TDC sensor is based on a capacitive measurement method. In this method, the changes in capacitance between the piston and the sensor head are measured by TDC sensor. The change in capacitance is inversely proportional to the gap between the piston and the sensor head. Figure 5.4 schematically presents the functional principle of a capacitive TDC sensor. Typically, a capacitive proximity sensor has two conductive plates separated by a dielectric material. An imbalance of electrical charges between the plates is created by applying a voltage difference. The capacitance determines the amount of current flow, which depends on the conductive plate proximity. In the capacitive TDC sensor, one conductive plate is the sensor probe, and another conductive plate is the piston (Fig. 5.4). The TDC sensor is installed in such a way that moving the piston does not touch the

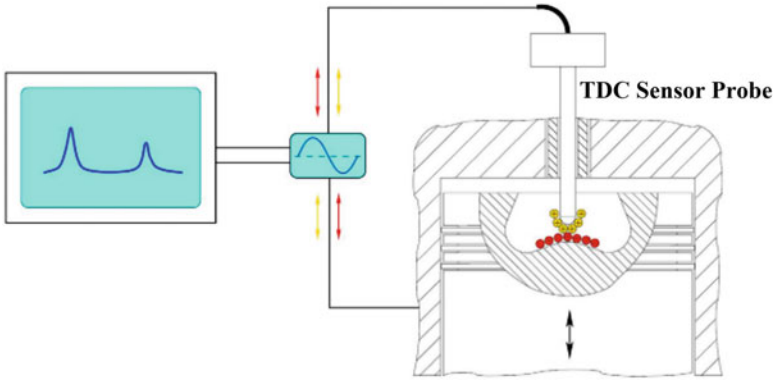

Fig. 5.4 Functional principle of capacitive TDC sensor [8]

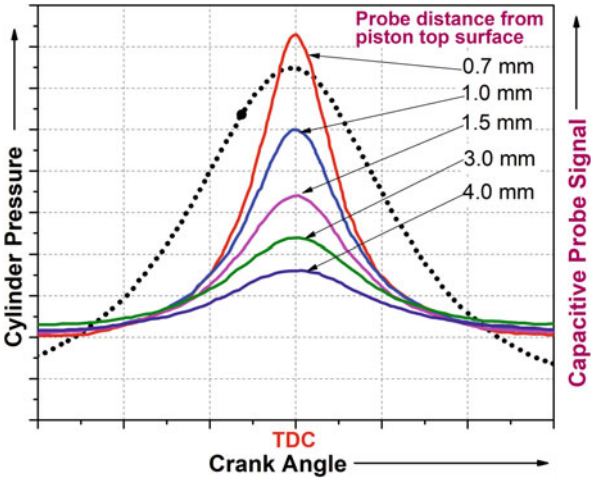

Fig. 5.5 TDC signal versus crank angle depending on the probe distance (Courtesy KISTLER)

sensor probe. The TDC sensor generates the signal with amplitude inversely proportional to the distance between the sensor tip and the piston top [8]. The maximum amplitude of the TDC sensor signal provides the exact location TDC. The output signal amplitude for compression conditions is lower in comparison to gas exchange conditions (Fig. 5.4). The lower amplitude during the compression conditions is caused by the cylinder pressure acting upon the engine components, which alters operating clearances [4]. Additionally, this phenomenon helps in discriminating compression TDC and gas exchange TDC positions.

Figure 5.5 presents the TDC signal as function of crank angle depending on the probe distance. The figure clearly illustrates that the signal amplitude depends on the distance between the probe and the piston. Minimal gap between the sensor probe and the piston is decisive for a good quality signal, but a certain gap must be present to prevent damage from touching of piston and sensor tip, which is typically between

0.5 and 1.5 mm [4]. The probe should be installed perpendicular to the piston crown in possible limits. This factor affects the choice of the measuring bore, and thus, if possible, the sensor should not be inclined more than 30° from the piston movement axis [4]. In order to determine the exact TDC position, the maximum amplitude of the TDC sensor signal must be evaluated. The TDC evaluation can be performed with great accuracy due to the high degree of symmetry of the signal (Fig. 5.5).

The TDC sensor is designed to measure the minimum clearance height, and thus, it is not always necessary to coincide with exact TDC position due to various factors such as bearing play and piston pin offset [4]. The output signal (analog voltage) of correctly installed TDC sensor is a smooth and symmetrical curve, which is typically used for TDC determination. Typically, the output signal is processed by indicating systems in connection with an angle encoder directly. The maximum position the TDC sensor's output signal cannot be used for the determination of the TDC location because the piston/crank movement is very small around TDC, which can lead to imprecise TDC sensing. Therefore, the "horizontal-cut principle" is used for calculation of TDC position, which is illustrated in Fig. 5.6. The output signal of TDC sensor is bisected at equidistant points before and after TDC, and the straight lines are connected from each symmetrical point. The center position is calculated from straight lines, and best fit line connecting to the multiple center points establishes the TDC position on the curve.

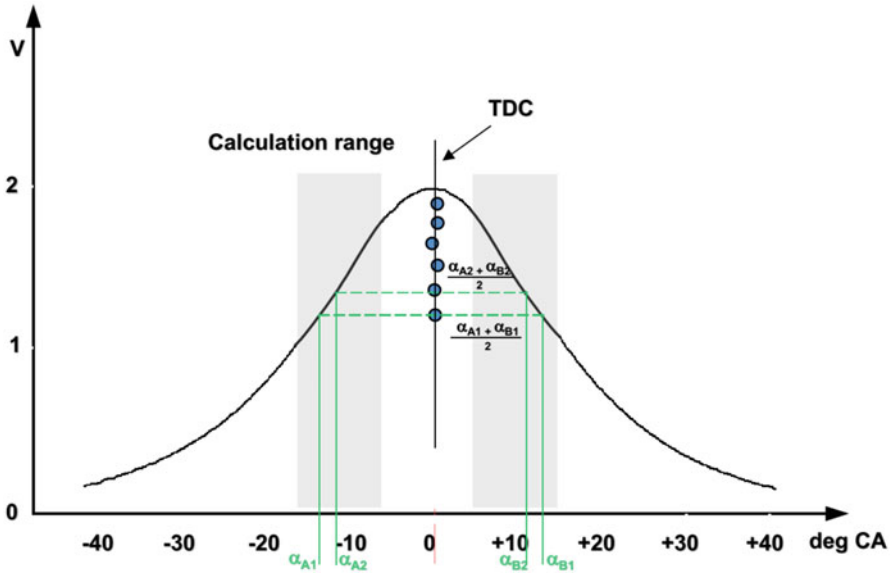

Fig. 5.6 Illustration of horizontal-cut principle for TDC determination in reciprocating engines (Courtesy AVL)

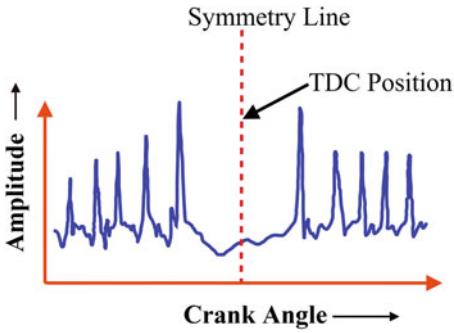

Fig. 5.7 Typical microwave signal near TDC (Adapted from [10])

5.2.1.3 Microwave Probe

Microwave detection is another method for determination of dynamic TDC position in a reciprocating engine via piston movement [9, 10]. In this method, low-power microwaves are used to determine the piston proximity and movement. The measurement system measures the output signal with respect to crank position. A computer-controlled variable frequency oscillator (VFO) enables the measurement system to be utilized with a wide range of cylinder displacements. The uniqueness of the microwave measurement process is the ability to accurately determine TDC position in real time, with the engine running (or cold-motored) at virtually any engine speed [4].

In this method, the combustion chamber of the engine is treated as a variable-length microwave resonator. The TDC position is established by investigating a series of resonance location data that is recorded as a function of crank angle position. The probe couples the microwave with the engine combustion chamber and determines the reflection coefficient of the microwave signal. The structure of the probe is similar to a miniature whip antenna used on automotive vehicles [9]. The probe, pre-chamber (in case of IDI engine), and cylinder comprise a microwave cavity which is tuned by the piston position. Reflected signals from the cavity vary in amplitude as the piston ascends in the compression stroke and descends in the power stroke as shown in Fig. 5.7. Each peak position on the microwave signal corresponds to the microwave resonance frequency for the mode. The detected microwave signal shows a peak at every resonance dip because a detector with a negative output signal was used. In principle output signal should be symmetrical with respect to TDC. The TDC can be determined by calculating the center of symmetry (Fig. 5.7) [10].

5.2.2 Phasing Methods Using Measured Pressure Data

Measured in-cylinder pressure-based methods for dynamic TDC determination are well established and typically supported by all cylinder pressure measurement equipment. This method of TDC determination does not require any additional

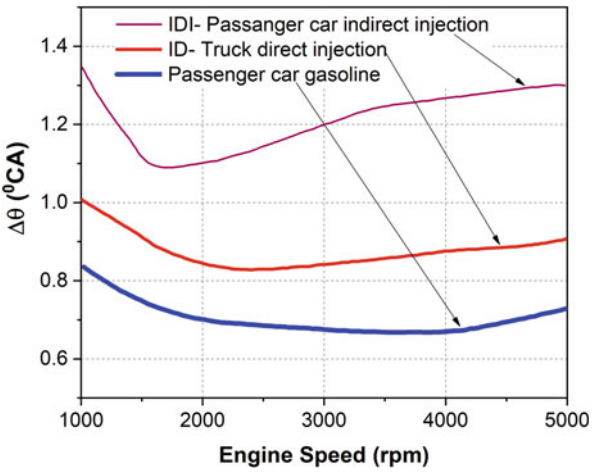

Fig. 5.8 Typical thermodynamic loss angles for different engines (Courtesy AVL)

hardware other than cylinder pressure sensor, which is anyway present for combustion analysis. Most of the methods use motored (unfired) cylinder pressure as a function of crank angle position for TDC determination. In ideal conditions (absence of heat transfer and mass losses), the peak pressure must occur at TDC position during unfired engine operating condition due to lowest cylinder volume at TDC position. Hence, the position of motoring peak cylinder pressure can be assumed as TDC position. However, in real conditions, the heat transfer and mass losses cannot be avoided. The peak pressure position occurs before real TDC position due to wall heat transfer and mass losses in real engine operating condition (Fig. 5.1). The difference between the peak pressure position and the actual TDC position is defined as the thermodynamic loss angle. The loss angle depends on a number of operating conditions (engine speed, temperature, blowby, etc.). Figure 5.8 depicts the thermodynamic loss angle as a function of engine speed for different engine combustion modes. The figure shows that the thermodynamic loss angle is higher at lower engine speeds because higher time is available for heat transfer at lower engine speeds.

Thermodynamic loss angle can be calculated by comparing the TDC sensor and the unfired cylinder pressure signals. However, this method of calculation of loss angle requires the additional hardware (TDC sensor) and its installation. Several algorithms are proposed in the published literature to calculate the thermodynamic loss angle only by measured pressure signal. The TDC determination methods based on polytropic exponent, symmetry of pressure curve, loss function, temperature-entropy diagram, inflection point, and IMEP-based calibration using measured cylinder pressure are presented in Sect. 10.1 of Chap. 10.

The accuracy of the TDC position depends on the estimation method. The application of particular method involves significant effort, cost, and time. Figure 5.9 shows the accuracy of different TDC determination methods with time and effort required. The static TDC determination method involves minimal expanse but considerable effort. This method is able to estimate reasonably accurate TDC

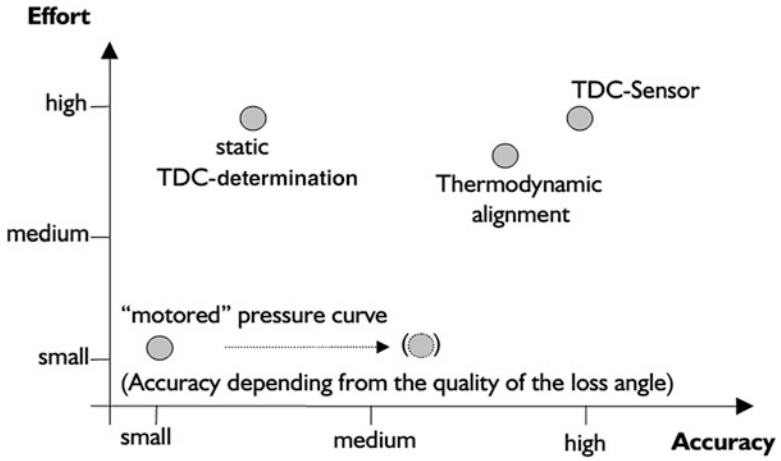

Fig. 5.9 Accuracy of different TDC determination methods with time and effort (Courtesy AVL)

position, but this does not account for dynamic effects. The TDC determination using the TDC sensor provides the most accurate TDC position estimation, but it also involves significant cost and effort. The motoring pressure-based estimation of TDC position has the accuracy depending on the algorithm used for calculation of thermodynamic loss angle.

5.3 Absolute Pressure Referencing (Pegging)

The quartz piezoelectric pressure transducers have been commonly used for the measurement of the cylinder pressure in reciprocating engines due to the advantages of good thermal performance and durability, high-frequency response, small size, light weight, large measuring range, etc. Inherent characteristics (working principle) of piezoelectric transducers require referencing of the output signal to absolute pressure (pegging). The piezoelectric pressure transducers can only measure the changing pressure content, i.e., only pressure variations in the combustion chamber, and not the physically correct absolute value of pressure in the combustion chamber. The charge output from the piezoelectric pressure sensor is supplied to the charge amplifier, which converts the charge output to a proportional voltage signal (see Chap. 2). The voltage signal is recorded by data acquisition system into digital format. The recorded voltage can be converted into absolute cylinder pressure data by Eq. (5.1) [11, 12]. This equation assigns a known absolute pressure value at particular pegging position in the engine combustion cycle:

$$P(\theta) = P_{\text{peg}} + \text{cal}\left[v_{\text{t}}(\theta) - v_{\text{t}}\left(\theta_{\text{peg}}\right)\right] \tag{5.1}$$

where P_{peg} is the known absolute pressure value at the pegging position, "cal" is calibration factor of the transducer (bar/Volt), v_t is the measured voltage, and θ_{peg} is the crank angle position of pegging point. In case of the noisy signal, it is important to use the average value of multiple points (10–15) at the pegging position to estimate $v_t(\theta_{peg})$, as presented by Eq. (5.2):

$$v_t(\theta_{peg}) = \frac{1}{w}\sum_{z=-k}^{k} v_t(\theta_z) \quad \text{where } k = \frac{w-1}{2} \tag{5.2}$$

Pegging position depends on the point, where the user can provide a known absolute pressure value. Typically, two parameters, i.e., the intake manifold absolute pressure or exhaust backpressure and the polytropic exponent, are mainly used to correct the measured cylinder pressure signal. Absolute pressure referencing (correction) may also be required to compensate for inter-cycle and intra-cycle drift (long-term and short-term drift, respectively) which necessitates individual cycle referencing [13]. The cylinder pressure curve would drift more or less globally if it isn't corrected because the piezoelectric transducers can only measure the relative variations of cylinder pressure. Figure 5.10 shows the measured in-cylinder pressure curves of two cylinders from an eight-cylinder diesel engine, where one cylinder pressure is corrected using fixed polytropic exponent. The cylinder pressure curve for cylinder 5 is obviously unreasonable (Fig. 5.10) because both the two cylinders are in the normal working state and the curve of cylinder 1 has been already corrected. The reason is that the pressure curve of cylinder 5 drifts globally based on an arbitrary ground under the effect of the disadvantages of the quartz piezoelectric pressure transducers [14]. Therefore, the measured in-cylinder pressure signal by the piezoelectric transducers must be correctly referenced to get authentic combustion pressure data.

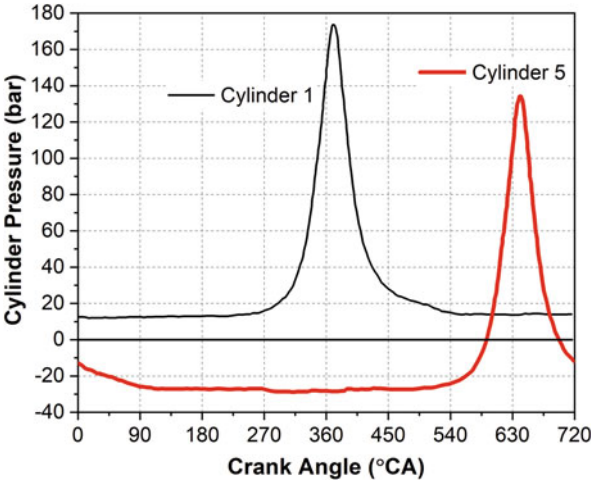

Fig. 5.10 Pressure curves of cylinder 1 and cylinder 5 from an eight-cylinder turbocharged diesel engine (Adapted from [14])

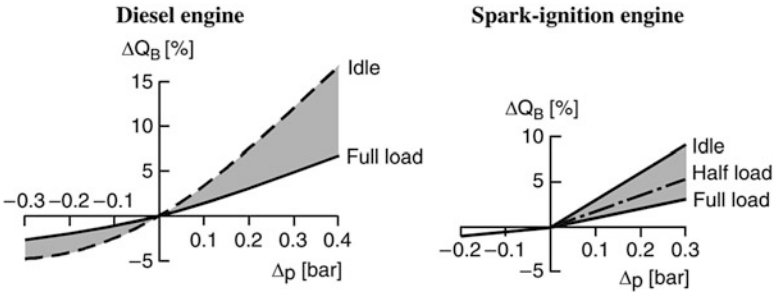

Fig. 5.11 Effect of referencing error in absolute pressure value on the energy balance [15]

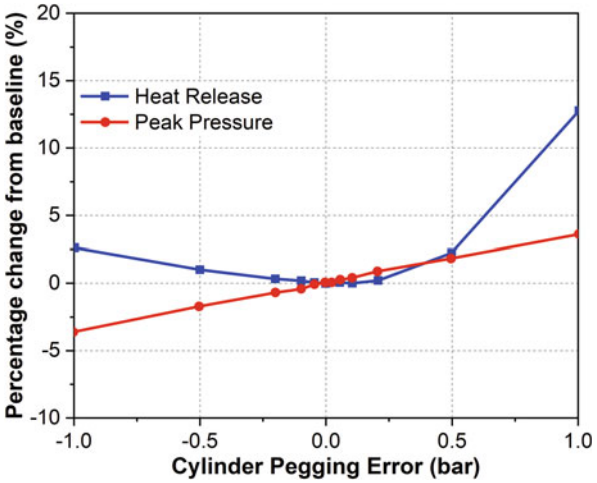

Fig. 5.12 Effect of referencing error on cumulative heat release and peak pressure in a stoichiometric non-dilute operating condition at 2000 rpm (Adapted from [16])

Incorrect pegging or absolute pressure referencing can affect calculated combustion parameters such as the heat release energy and heat release rate, mass fraction burned and burned angles, compression and expansion polytropic indices, estimated pressure drop across ports, estimated cylinder charge mass, estimated charge temperature and derived quantities, etc. Figure 5.11 shows the referencing error on energy balance in SI engine and diesel engine. A positive referencing error ($+\Delta p$) leads excessive cylinder pressure (and vice versa), which results into smaller conversion rates before the TDC position and to larger ones after the TDC. Since most of the heat conversion takes place after the TDC, most of the changes occur in this part of the combustion sequence [15].

Most parameters are essentially unaffected for reasonably small errors in pressure referencing. Typically, IMEP is unaffected by absolute pressure corrections because it is a cycle-integrated parameter and shifting the pressure values does not change the area contained in the pumping or compression/expansion loops [16]. Figure 5.12 shows the effect of pegging error on cumulative heat release and peak pressure in a stoichiometric non-dilute operating condition at 2000 rpm. The figure shows that the

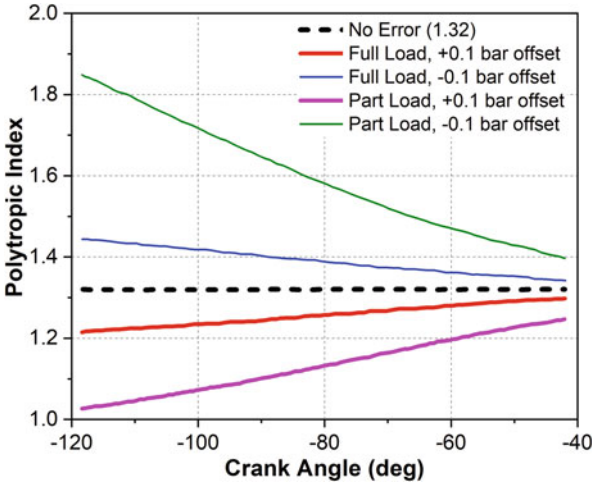

Fig. 5.13 Effect of ±0.1 bar pegging errors on the calculated compression polytropic exponent at part-load and full-load operating condition (Adapted from [13])

calculated heat release in the engien cycle is increased by over 10% for the case of the pegging error of 100 kPa, but for all other cases, the effect is much more modest. However, the peak pressure is shifted by exactly the amount of the pegging error, as would be expected.

Figure 5.13 shows the effect of ±0.1 bar absolute pressure offsets on the estimated compression polytropic exponent using simulated engine pressure data at part-load and full-load operating conditions. The simulated data were generated by assuming a fixed polytropic index of 1.32 throughout the compression process. Figure 5.13 depicts that a low polytropic exponent is calculated when the pressure is too high, and the error in the polytropic exponent is more sensitive to a specified magnitude of pressure error at low engine load. Additionally, the largest polytropic index errors are incurred early in the compression process (Fig. 5.13) and that the erroneous polytropic indices vary greatly with crank angle.

Cylinder pressure-based charge temperature calculations are often used to calculate the mean gas temperature and derived parameters such as wall heat flux, gas properties, and component temperatures. A study showed that the calculated temperature is very sensitive to pressure referencing, and with a −0.1 bar error at low-load operating condition can lead to a change in peak temperature of 1000 K. At full load, the same magnitude of pressure error would still cause a 250 K shift in peak temperature [13].

For achieving good accuracy in the derived parameters, the accurate pressure pegging is highly desirable for both mean cycle and individual cycles. A certain level of referencing errors will always be present. However, in practice referencing errors need to be reduced to an acceptable limit. The minimum pressure referencing accuracy required depends on the type of analysis being performed and the engine operating conditions [13]. Higher absolute pressure accuracy is typically required for combustion analysis at low engine load and under slow burn conditions. High referencing accuracy around the whole combustion cycle can only be attained

in the absence of all other sources of pressure measurement error. Thermal shock, long-term drift, and sensitivity errors mean that correct pressure referencing will only occur over a limited portion of the engine cycle. For example, thermal shock can distort the pressure by a variable amount over most of the engine cycle. In this condition, the accurate pressure referencing becomes difficult, and it is necessary to decide which part of the engine cycle needs to be most accurately referenced.

Several methods are proposed in published literature for absolute pressure correction including (1) pegging to intake manifold pressure near intake BDC using absolute intake manifold pressure sensor, (2) pegging to exhaust manifold pressure near exhaust TDC using absolute exhaust manifold pressure sensor, (3) referencing by an absolute cylinder pressure sensor exposed to the cylinder charge near to BDC, (4) installing a switching adapter to expose the piezoelectric sensor to a known pressure during part of the engine cycle, and (5) using a numerical referencing method based on polytropic index (constant or variable) [13]. Each of these approaches has advantages and disadvantages and an expected level of accuracy. An iterative method for determining the pressure offset is proposed using the tuning of heat release curve during motoring condition or compression phase of firing condition [17]. In this method, it is assumed that no heat is released during the compression phase or motoring condition, and the zero line can be corrected until this requirement is met. However, this method has the disadvantage of the enormous amount of computation, and it also requires corrected parameters used in heat release calculation. The commonly used methods for absolute pressure referencing are discussed in the following subsections.

5.3.1 Inlet and Outlet Manifold Pressure Referencing

Manifold pressure pegging has the advantage of relative simplicity but does require additional pressure transducer. Manifold pressure sensors are ideally required one per cylinder mounted in each runner, and water-cooled for exhaust pressure transducers [13]. Intake manifold pressure sensors are mostly absolute pressure sensors and have a high accuracy of approximately ± 10 mbar. The combustion chamber pressure can be adjusted to the intake manifold pressure if the flow in the cylinder is balanced. An appropriate time for this is the BDC position of the intake stroke because the piston speed is zero at this position. However, under highly tuned operating conditions, improper selection of the measurement point (or the use of a pressure transducer with inadequate frequency response) will introduce systematic errors [18]. Thus, intake manifold pressure referencing (IMPR) is an appropriate method for an untuned intake system or a tuned system which has a very low engine speed. Additionally, the measurement noise at intake BDC position can lead to incorrect referencing results for the all pressure data points of the engine cycle. Even if the average value of several points near intake BDC position is used for referencing, this method still has error with a tuned intake system or at high engine speed [19, 20].

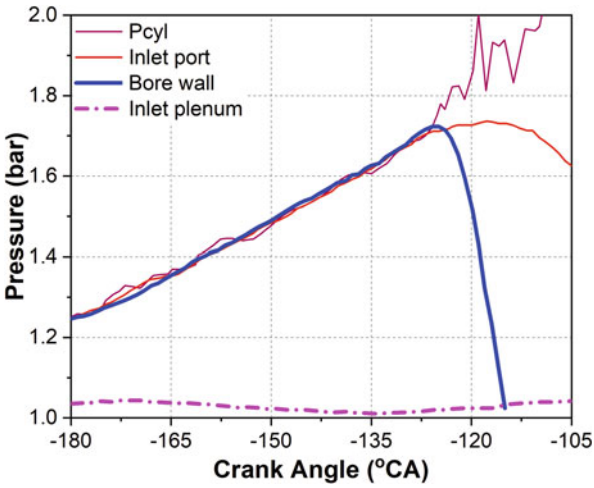

Fig. 5.14 Different pressure signals as a function of crank angle (Adapted from [18])

Intake manifold pressure sensor can be mounted centrally in the intake manifold so that all cylinders use the same pressure value before the intake ports for correction, or the pressure sensor can be mounted in each inlet port of a cylinder near the intake valve, which removes cylinder-specific differences. The most accurate but also the most expensive method is to mount a sensor in each inlet runner. A study mounted three absolute pressure sensors in (1) the inlet plenum, (2) the inlet port 7 mm above the valve seat, and (3) through the bore wall such that the transducer is 5 mm above the piston at BDC for pressure referencing [18]. Figure 5.14 shows the measured pressure signal at each of these positions. The figure clearly depicts that the common method of pegging to the pressure measured in the inlet plenum will introduce systematic errors when manifold tuning is significant. Additionally, the pressure measured in the inlet port close to the valve seat precisely follows the pressure measured through the bore wall, up to the point where the piston covers the transducer hole (at -126° BTDC). Access to the inlet port is typically much more convenient than through the bore wall.

In practice, the intake BDC is used for pressure referencing position. However some dependence on the crank angle position used for the referencing would be expected. Figure 5.15 shows the change in pressure referencing by varying the crank angle over which the referencing is performed (datum value is BDC, ± 10 crank angle degrees average in all cases). The figure shows that changing the position for intake manifold pressure referencing (IMPR) does produce a sizeable change in the absolute pressure. A later referencing crank angle initially increases the absolute pressure (Fig. 5.15). As expected, the variations with crank angle position are greatest for the higher flow rate cases. The best location for pressure referencing is reasonably the flat portion of the curve where the manifold and cylinder pressures are the same or have a constant difference. The study concluded that pressure referencing at 10–15° after BDC position is optimum for this engine [13].

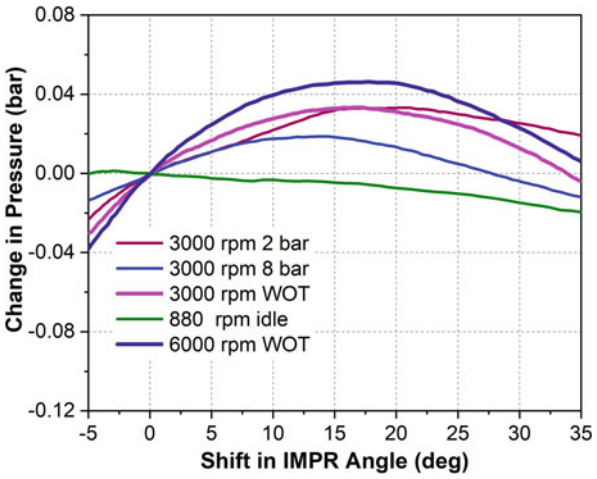

Fig. 5.15 Effect of manifold pressure sensor referencing crank angle position on referencing pressure (Adapted from [13])

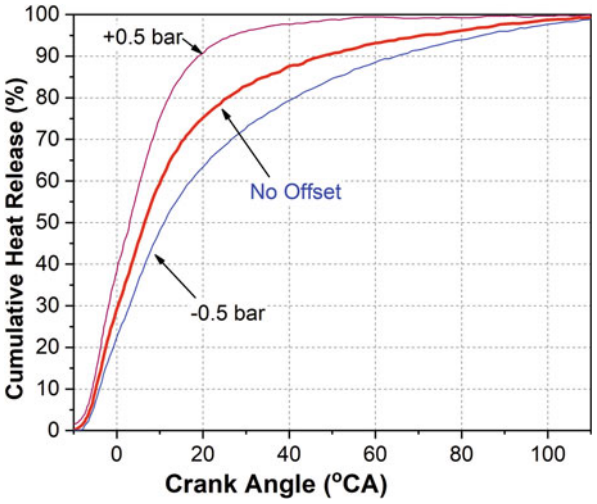

Fig. 5.16 Cumulative release curves with different pressure offset values (Adapted from [14])

The global drift of the cylinder pressure curve not only leads to wrong values of the whole engine cycle but also leads to the wrong calculation of combustion parameters. Figure 5.16 shows the cumulative heat release curves calculated from the measured cylinder pressure with different cylinder pressure offsets. The cumulative heat curves vary with the changes of cylinder pressure offsets, and in case of $+0.5$ bar offset, the heat release rate increases more rapidly with the increase of the crankshaft angle when compared with the curve with no offset (Fig. 5.16). The study showed that the ± 0.5 bar offset could lead to up to 45% error in the calculation of combustion duration [14]. Thus, a proper correction method of cylinder pressure is the prerequisite for the analysis of the combustion process in reciprocating engines.

In the outlet pressure referencing method, the cylinder pressure during the exhaust stroke (typically TDC position or average pressure during exhaust stroke) is assumed to be equal to the exhaust backpressure. The pressure fluctuations of the exhaust manifold are more noticeable than those of the intake manifold [19]. Averaging the pressure data over several crank angle degrees can reduce the effect of this fluctuation and the measurement noise. However, an additional pressure sensor is required for exhaust backpressure measurement that can be used for pegging/referencing.

5.3.2 Two- and Three-Point Referencing

In two-point method, a fixed polytropic coefficient is assumed. In this method, cylinder pressure offset is calculated using measured cylinder pressure data at two points $\theta(i)$ and $\theta(i + 1)$ in the compression stroke (Fig. 5.17). The points are considered before the start of combustion and after the intake valve closing. The compression process in the engine is considered as polytropic compression process (PV^n = constant) before the start of combustion during the compression stroke. Thus, polytropic expression at two points can be written as Eq. (5.3) [21]:

$$\begin{aligned} &P_{\text{cyl}}(i+1) = P_{\text{cyl}}(i) \cdot \Omega(\text{i})^n \\ &\text{With} : \Omega(i) = \frac{V(i)}{V(i+1)} \end{aligned} \tag{5.3}$$

The true cylinder pressure (P_{cyl}) and measured cylinder pressure (P_{m}) are related to pressure offset (P_{offset}) by Eq. (5.4):

$$P_{\text{cyl}} = P_{\text{m}} + P_{\text{offset}} \tag{5.4}$$

In this method, the polytropic exponent is assumed to be known, and the pressure offset is constant. Thus, the pressure difference (ΔP) between two points of the

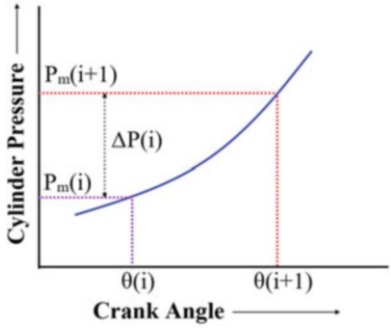

Fig. 5.17 Compression cylinder pressure of the reciprocating engine

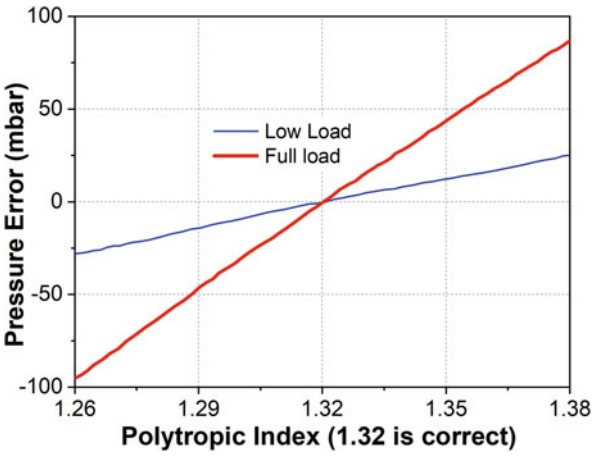

Fig. 5.18 Sensitivity of calculated absolute pressure to the assumed polytropic exponent (Adapted from [13])

cylinder pressure curve (Fig. 5.17) must be independent from the pressure offset value:

$$\Delta P(i) = P_{\mathrm{m}}(i+1) - P_{\mathrm{m}}(i) = P_{\mathrm{cyl}}(i+1) - P_{\mathrm{cyl}}(i) \tag{5.5}$$

By using Eqs. (5.3) and (5.5), the pressure offset can be calculated by Eq. (5.6):

$$P_{\mathrm{offset}} = P_{\mathrm{m}}(i) - \frac{\Delta P(i)}{\Omega(i)^n - 1} \tag{5.6}$$

Typical values of the polytropic exponent for CI and SI engines in motoring operation are $n = 1.37$–1.40, and for SI engines with a stoichiometric air-fuel ratio condition $n = 1.32$–1.33 [15].

Figure 5.18 shows the relationship between the assumed polytropic exponent and the absolute pressure referencing error for the case of simulated pressure data based on $n = 1.32$. The figure shows that errors in the fixed polytropic exponent of ± 0.05 cause referencing errors of typically ± 75 and ± 25 mbar for full-load and part-load conditions, respectively. The fact that the errors are proportional to load is favorable for combustion analysis because larger referencing errors can normally be tolerated at higher load [13].

Considering the error in the assumed polytropic exponent, it can be calculated as well from the measured pressure data. Thus, the pressure offset and polytropic exponent are the two unknown parameters which can be calculated from two independent equations. For generating two equations, an additional point can be considered in the compression stroke. This method is called three-point referencing method. Two equations are created in the same way as Eq. (5.6) with three points from the measured cylinder pressure signal in compression stroke as Eq. (5.7) [21, 22]:

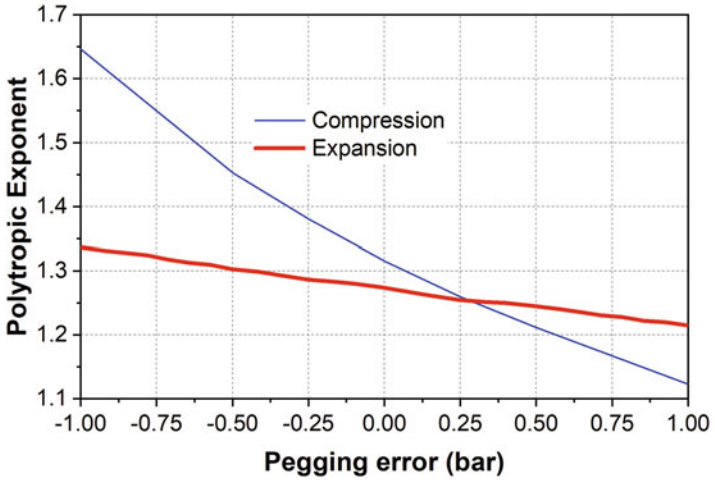

Fig. 5.19 Effect of pegging errors on compression and expansion polytropic coefficients (Adapted from [18])

$$\frac{P_{\mathrm{m}}(i+1)-P_{\mathrm{m}}(i)}{\left(\frac{V(i)}{V(i+1)}\right)^{n}-1}=\frac{P_{\mathrm{m}}(i+2)-P_{\mathrm{m}}(i)}{\left(\frac{V(i)}{V(i+2)}\right)^{n}-1} \tag{5.7}$$

Equation (5.7) cannot be solved analytically to determine the polytropic exponent "n." Therefore, it is solved iteratively by writing in the form $n = f(n)$. Successively, the cylinder pressure offset can be calculated by polytropic exponent using Eq. (5.6). The study used state space formulation to determine the pressure offset and polytropic exponent using tow extended Kalman filters [21].

Figure 5.19 shows the effect of pegging errors on the calculated values of compression and expansion polytropic coefficients. The effect of pegging errors is more pronounced on the compression metric than the expansion (Fig. 5.19) due to the expansion occurring at a much higher pressure, making a given pegging error a smaller percentage of the values used to calculate the coefficient. Figure 5.20 shows the effect of pegging errors on burn locations (10%, 50%, and 90%) using actual calculated as well as forced (assumed) polytropic coefficients. The figure depicts that a -2° error in CA50 per bar of pegging error when the heat release algorithm uses the actual calculated polytropic coefficients. Figure 5.20 also depicts a $+2.3^{\circ}$ error in CA50 per bar of pegging error when the using assumed (forced) polytropic coefficients [18].

In this method, referencing errors mainly produced from disturbed measured values and an incorrect determination of the polytropic exponent. Moreover, this method can only give correct results if the thermal shock remains constant between the two sampling points.

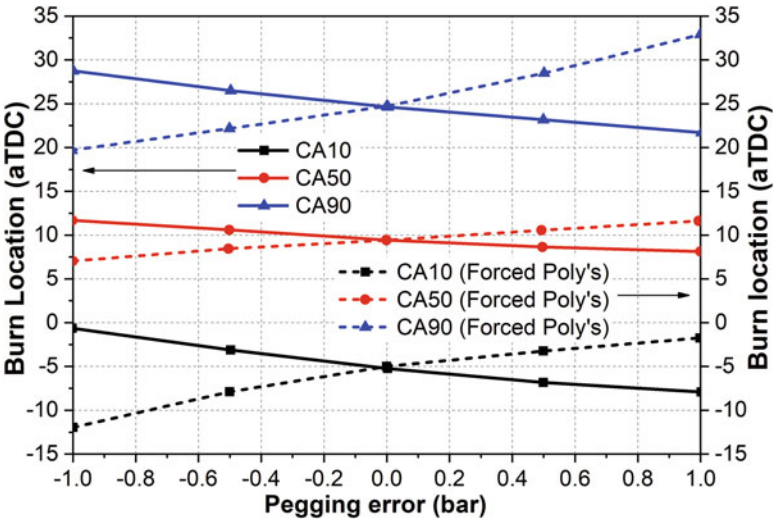

Fig. 5.20 Effect of pegging errors on burn locations using calculated and assumed polytropic coefficients (Adapted from [18])

5.3.3 Referencing Using Least-Square Methods

In order to reduce the sensitivity of measurement, the pressure sensor offset voltage is determined by evaluating a number of measurement samples (instead of two or three) and applying regression calculations. Typically, more than two measurement samples of the cylinder pressure signal are available during the compression process. The measured voltage during the compression phase or motoring engine operation can be written as Eq. (5.8) [19, 20]:

$$\begin{aligned} E(\theta) &= K_S \cdot c(\theta) \cdot p(\theta_{ref}) + E_{bias} \\ c(\theta) &= \left[\frac{V(\theta_{ref})}{V(\theta)}\right]^k \end{aligned} \tag{5.8}$$

where E is voltage; K_S and E_{bias} refer to the sensor gain and sensor offset voltage, respectively; and $V(\theta_{ref})$ and $p(\theta_{ref})$ represent cylinder volume and pressure at a reference crank angle.

The Eq. (5.8) can be written in matrix form as Eq. (5.9):

$$y = X \cdot w \tag{5.9}$$

where

$$y = \begin{bmatrix} E(\theta_1) \\ E(\theta_2) \\ \vdots \\ \vdots \\ E(\theta_N) \end{bmatrix}, \quad X = \begin{bmatrix} 1 & c(\theta_1) \\ 1 & c(\theta_2) \\ \vdots & \vdots \\ \vdots & \vdots \\ 1 & c(\theta_N) \end{bmatrix}, \quad w = \begin{bmatrix} E_{\text{bias}} \\ K_S \cdot p(\theta_{\text{ref}}) \end{bmatrix} \tag{5.10}$$

Applying the linear least-square method, the parameter vector can be calculated as Eq. (5.11):

$$w = \left(X^T X\right)^{-1} X^T y \tag{5.11}$$

Since the sensor gain is already known, the sensor offset voltage and the reference cylinder pressure can be calculated simultaneously by Eq. (5.11).

The least-square method (LSM) is considered the best method for pegging the measured cylinder pressure [13]. This method assumes a polytropic coefficient, and it is becomes unsuitable when the polytropic coefficient is unknown. Similar to the two-point referencing method, this method also has a drawback of the assumption of a fixed polytropic coefficient. Therefore, an erroneous choice or changes of the polytropic coefficient can lead to pegging error [19]. Therefore, sensor offset voltage estimation by using the least-square method with the variable polytropic coefficient is proposed [19, 20]. This method has the assumption that the polytropic coefficient is slowly varying cycle-by-cycle and fixed during one cycle. The estimation of the polytropic coefficient on the *i*th cycle is derived using Eq. (5.12):

$$\tilde{k}_i = \frac{\ln\left[p(\theta)/p(\theta_{\text{ref}})\right]}{\ln\left[V(\theta_{\text{ref}})/V(\theta)\right]} \tag{5.12}$$

In order to achieve robustness of estimation, a first-order auto-regressive filter is applied to the estimation result:

$$\hat{k}_i = a \cdot \hat{k}_{i-1} + (1-a) \cdot \tilde{k}_i, \quad 0 < a < 1 \tag{5.13}$$

This approach alleviates the computational complexity and the sensitivity to polytropic coefficient error [19].

Least-square method (LSM) and two-point referencing methods have the demerit of assuming a fixed polytropic exponent, while three-point referencing uses calculated exponent, but it suffers from noise sensitivity. Figure 5.21 depicts the calculated polytropic exponent using three-point method and lease square with a variable polytropic exponent (modified LSM). The figure shows that both methods trace the tendency of a transition, and modified LSM method effectively determines the polytropic exponent. The modified LSM methods demonstrated the least sensitivity

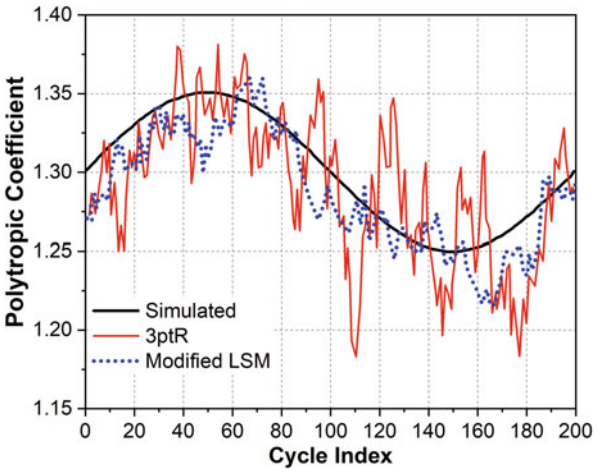

Fig. 5.21 Calculated polytropic exponents using three different methods [20]

to random noise [20]. Another model-based least-square method is proposed, which is computationally inexpensive, and well suited for real-time control applications [23].

5.3.4 Referencing Using Polytropic Coefficient Estimation

This method of pressure referencing also treats the compression stroke as a polytropic process and estimates the polytropic exponent. The polytropic exponent is a fixed value in the specified state, such as the same working condition in the particular engine, so that whole compression stroke seems to be adiabatic. However, in practical engine operating conditions, the adiabatic condition can only reach when cylinder charge temperature is close to the cylinder wall, which leads to the heat exchange close to zero. This condition occurs only in a certain crankshaft angle range during the compression stroke. Additionally, the loss of the charge through blowby can be neglected at the same time. Thus, crankshaft angle in this range can be used to analyze the curve of the polytropic exponent. A study found that the crank angle range for analyzing the polytropic exponent curve is between 80 °CA bTDC and 40 °CA bTDC for the turbocharged eight-cylinder diesel engine [14].

The polytropic exponent curve should be a horizontal line in the section of the compression stroke corresponding to the angle which can be regarded as the adiabatic process. However, if the curve is not a horizontal line, the cylinder pressure curve would experience global drift. In this case, the cylinder pressure curve needs to be added or subtracted by a fixed offset until the polytropic exponent curve becomes a horizontal line. In this process, the value of the polytropic exponent is calculated, and the cylinder pressure curve can be corrected simultaneously [14].

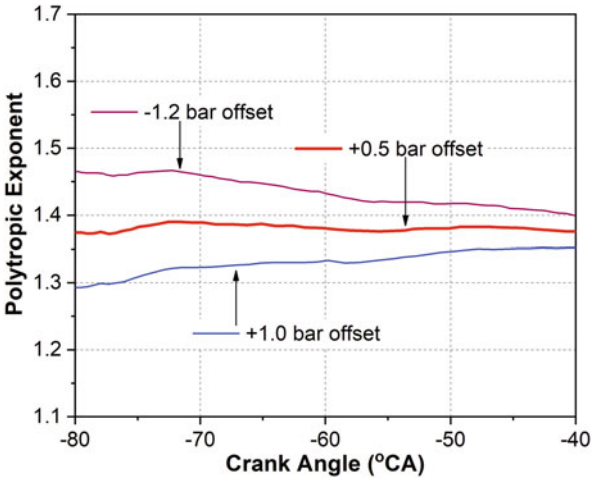

Fig. 5.22 Polytropic exponent curves with different offsets (Adapted from [14])

Figure 5.22 depicts the polytropic exponent curves calculated by the cylinder pressure curves with different offsets. The bigger the slope of the polytropic exponent curve is obtained for, the higher the offset of cylinder pressure (Fig. 5.22). Typically, the polytropic exponent should not be bigger than 1.4 in the adiabatic process. For the cylinder pressure offset of +0.5 bar, the polytropic exponent curve is a horizontal line, and the value of the polytropic exponent is not bigger than 1.4 in the analysis section. Therefore, the cylinder pressure curve corrected by +0.5 bar offset is the correct one, and the average value of the polytropic exponent curve in the angle analysis section is a correct polytropic exponent value. Thus, absolute pressure referencing of the measured pressure signal can be achieved using this method also.

5.4 Smoothing/Filtering of Experimental Data

Accurate measurement of in-cylinder pressure is clearly a prerequisite for good data and subsequent analysis. Typically, a large quantity of information related to the combustion process (heat release, combustion phasing, reaction rate, etc.) is generated by post-processing of the cylinder pressure signal. Therefore, it is essential to obtain actual physical information (cylinder pressure), which is free from signal noise. To conserve the useful physical information in the in-cylinder pressure signal, filtering (removal of high-frequency noise) or smoothing of the signal is necessary. Different filtering and averaging methods are generally used for smoothing the cylinder pressure signal, which leads to a precise combustion diagnosis [1, 2]. It is well known that differentiation (derivative) of signal leads to increase (amplification) of signal noise. Therefore, filtering the cylinder pressure signal is important because heat release calculation uses pressure derivatives. Signal noise present in the cylinder pressure data may lead to large error in heat release calculation. Figure 5.23 shows

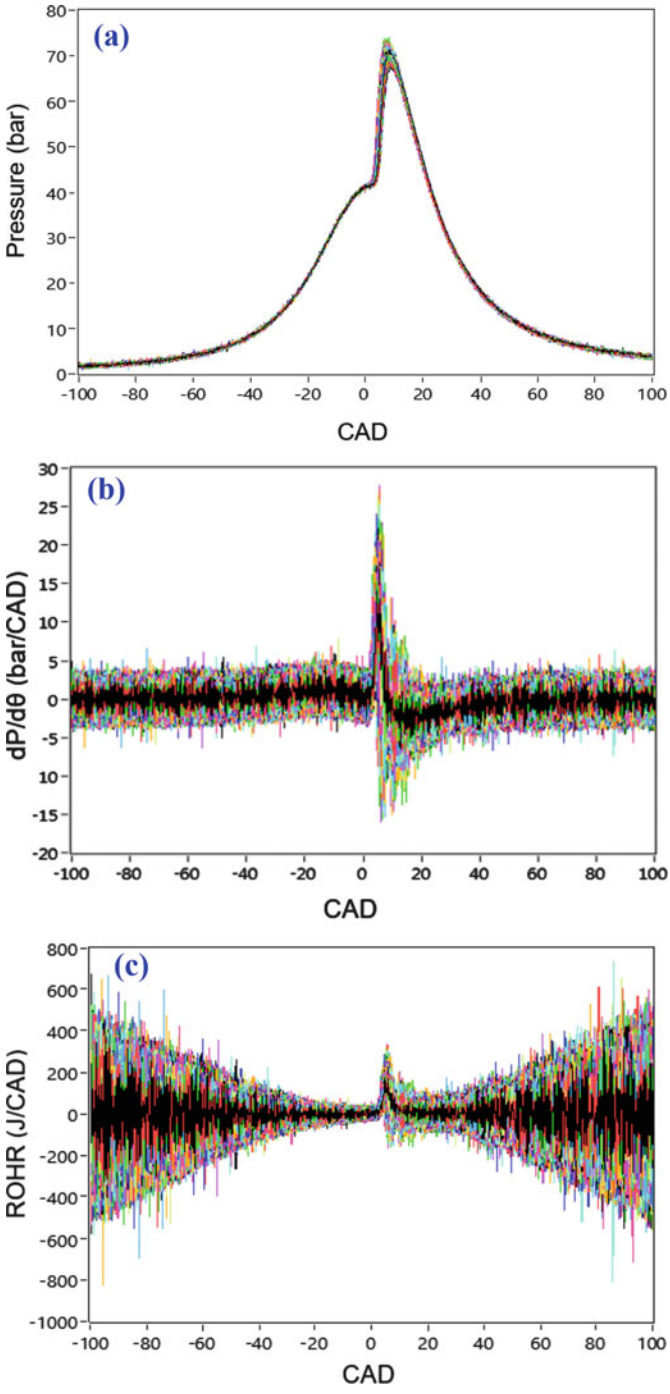

Fig. 5.23 (**a**) Measured cylinder pressure, (**b**) calculated pressure derivative, and (**c**) calculated heat release rate for 3000 consecutive cycles at 1200 rpm and $\lambda = 2.1$ in HCCI combustion engine [2]

the measured cylinder pressure signal and calculated pressure rise rate and heat release rate from the pressure signal for consecutive 3000 engine cycles in HCCI combustion engine at 1200 rpm. Cylinder pressure variations are maximum near TDC position (during combustion), and significant variation can be observed in peak pressure (Fig. 5.23a). Oscillations (variations) in pressure curves are relatively very small during the compression stroke in comparison to the variations during the combustion process in the engine cycle. Signal noise is not prominently perceived in the pressure curves. However, signal noise and cyclic variations are clearly perceived in calculated pressure derivative and heat release rate curves (Fig. 5.23a, b). Signal noise becomes amplified in the pressure derivative signal. Since heat release rate calculation involves pressure derivative, the heat release rate curves (Fig. 5.23c) has very high amplitude than the amplitude in the pressure curves (Fig. 5.23a). When the piston is away from TDC position, the heat release rate (Fig. 5.23c) is observed very high (where actually no heat release) due to signal noise in measured pressure signal. The possible reason for high heat release is that amplified signal noise gets multiplied by cylinder volume in heat release calculation. The cylinder volume as well as rate of change of cylinder volume is higher when piston is away from TDC position. This leads to a very large error in heat release rate calculation using noisy cylinder pressure signal.

There are several sources of signal noise in the measured pressure signal. Signal noise sources include the pressure conversion (non-flush sensor mounting, thermal effects, sensor resonance, lack of linearity in the sensor, vibrations, etc.), signal transmission (electrical effects, bad connections, etc.), and analog-digital conversion [1, 2]. Pressure waves caused by fuel injection or the rapid rate of premixed combustion or combustion chamber resonance are also recorded by the pressure transducer, which can cause errors in the calculation of heat release rate using first law of thermodynamics [24]. Variation in engine input parameters and variations in engine operating conditions also affect the measurement of the pressure signal and signal noise. Cyclic variations can even occur at steady-state engine operating conditions. The significance of this effect depends on the combustion modes such as SI, CI, or HCCI combustion.

Averaging of many engine cycles is suggested to reduce the errors in the processing of cylinder pressure due to signal noise. Averaging of cylinder pressure data for several cycles can only remove the random noise in pressure signal, and it cannot remove the systematic errors. Additionally, averaging several cycles is not suitable for the engine running under transient operating modes [24]. Averaging of cycles is also not possible when cyclic variations in the combustion parameters need to be analyzed. Averaging of pressure data can remove the random high-frequency noise from cylinder pressure signal. Figure 5.24 illustrates the removal of high-frequency noise by averaging different numbers of cycles in HCCI combustion data. The amplitude of power spectrum signal reduces with increase in number of averaging cycles (Fig. 5.24), which suggests that the averaging has reduced the random high-frequency noise.

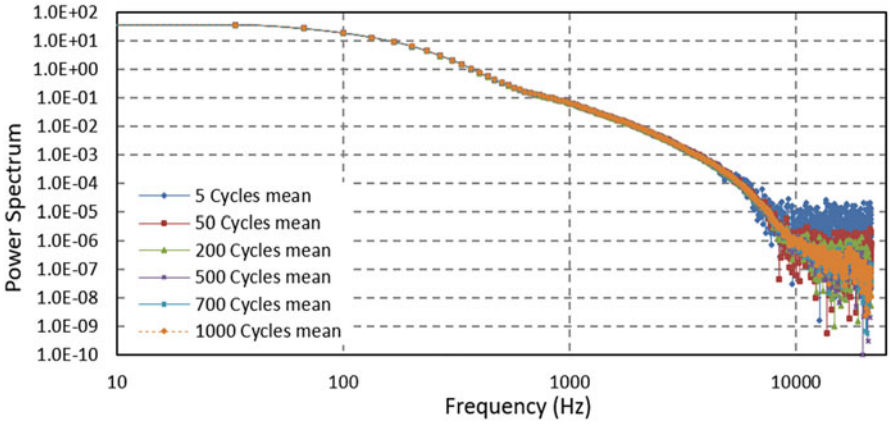

Fig. 5.24 Power spectrum of pressure signal for different numbers of cycles selected for averaging [2]

Filtering of signal noise is the only option in case of systematic errors and when averaging of the signal cannot be done. Even after averaging the pressure trace, it still requires filtering or smoothing after the premixed burn spike and the early pressure rise because of the effect of pressure waves initiated by combustion flame. Various filtering methods, such as moving average algorithms and low-pass FIR (finite impulse response) and IIR (infinite impulse response) filters, are discussed in next subsections of this section.

Another option to reduce the errors in heat release calculations is to directly measure the pressure derivative from the piezoelectric pressure sensor (see Chap. 2). This method is called current-to-voltage conversion, as rate of pressure change produces current that is converted into a voltage for data logging. Typically, cylinder pressure transducers, the charge is measured converted into voltage by the charge amplifier. This signal is used for computation of pressure derivative, where introduced signal noise gets amplified. Figure 5.25 presents the normalized heat release rate and mass fraction burned as a function of the crank angle measured by the current-to-voltage converter and charge amplifier. Figure 5.25a depicts that the heat release calculation has higher noise level in case of charge amplifier. Additionally, mass fraction burn calculation also affected by signal noise contains in the pressure signal measured using charge amplifier. It is shown that conversion of current produced from the piezoelectric transducer into an analog voltage signal reduces the quantization noise of pressure derivative data by about 70 times [25]. Various filters have been developed and recommended for filtering the signal noise to fulfill different requirements of processing the cylinder pressure for combustion diagnostics.

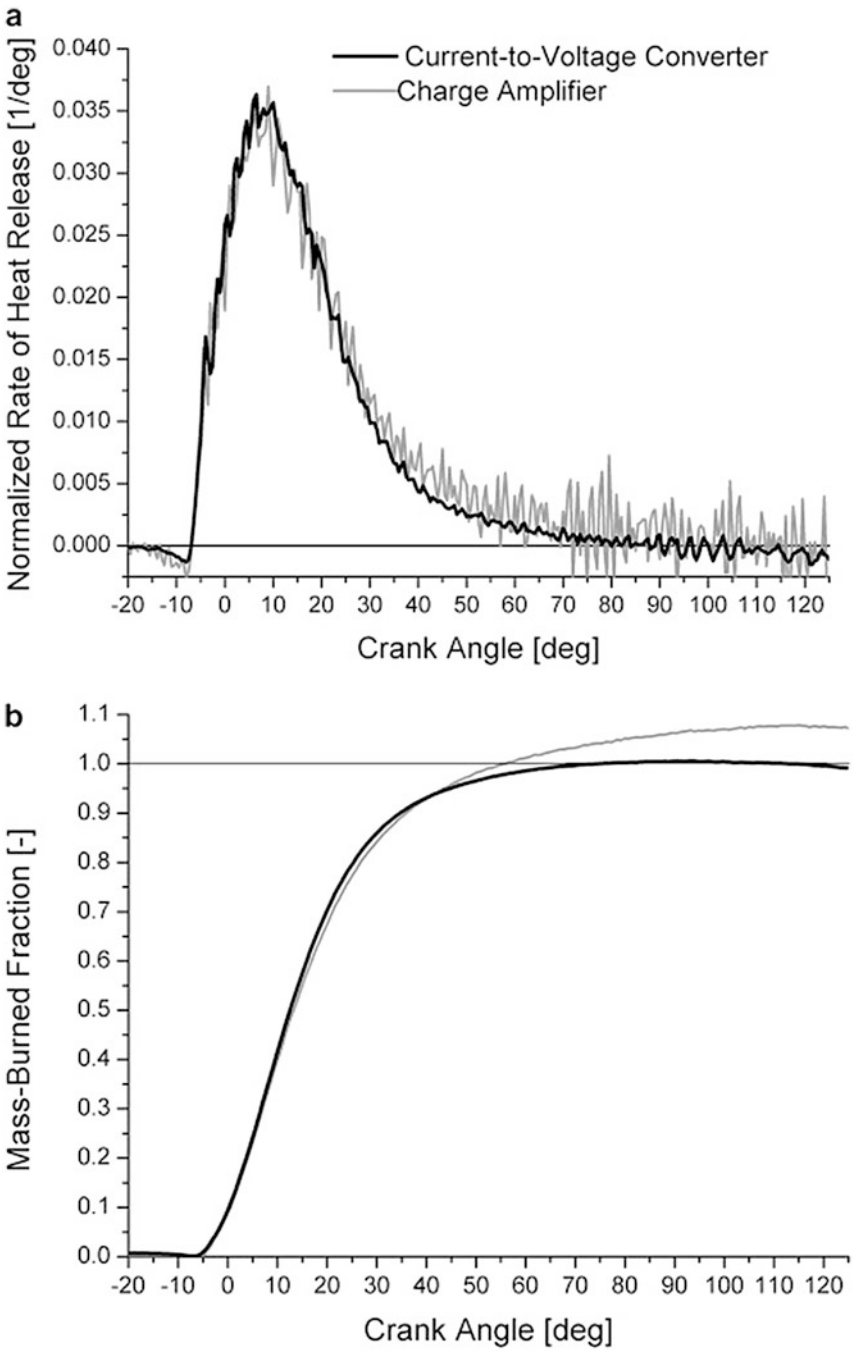

Fig. 5.25 (**a**) Normalized heat release rate, and (**b**) mass fraction burned as function of crank angle at full load [25]

5.4.1 Moving Average Filters

Cylinder pressure signal quality can be further improved by filtering and smoothing the experimental raw data. In some applications, filtering is targeted at much higher frequencies than the smoothing. For studies in which the frequencies of interest are the primary knock frequency and below, the data should be low-pass filtered at 30–50 kHz before digitization by high speed data acquisition system. Most charge amplifiers are equipped with an integral filter in this range. Smoothing is performed on the digitized data and can be successfully achieved using either the 3-point, 5-point, or 7-point least-square smoothing algorithms [24, 26]. Simple smoothing filters (such as a moving average or median filter) are frequently applied for decreasing the short-term signal fluctuations and estimating the long-term trend of the measured signal. The unweighted moving average filter can serve as a low-pass filter, and it uses the simplest convolution operation. More complex smoothing of measured signal with a weighted moving average is accomplished by applying the Savitzky-Golay convolution coefficients that can be computed from the least-square fit of subsets of adjacent data points with a low-degree polynomial [27].

Figure 5.26 presents the pressure signal filtering using four simple filters. Moving average filter with 5 and 10 data points spans, third-order polynomials for 1D median filter, and Savitzky-Golay filter with second-order polynomial with 7 points are used for smoothing (Fig. 5.26). Savitzky-Golay and the median filters show very good agreement with the raw data during compression stroke up until the start of combustion. The pressure curves with moving average filters deviated from measured raw data shortly before the initial pressure rise because of calculated average pressure in the window spread the effect of the quick pressure rise. Larger points moving average filter have the larger deviation as expected (Fig. 5.26). The high-frequency pressure signal noise generated during combustion is not eliminated effectively by any of the four filters. The worst performance is shown by median

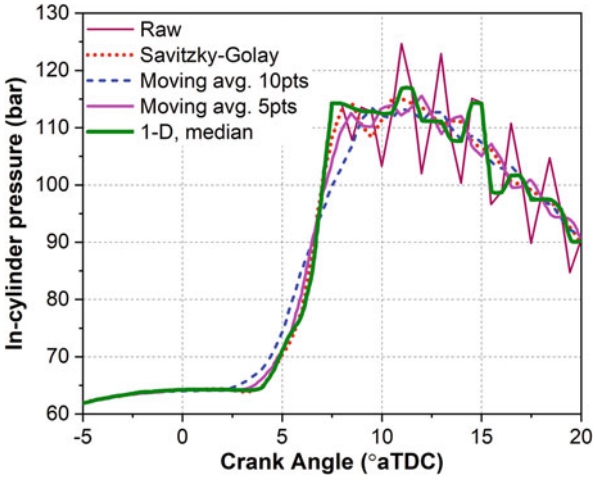

Fig. 5.26 Illustration of cylinder pressure signal smoothing using simple filters (Adapted from [27])

filter. Savitzky-Golay filter also exhibited higher oscillation in comparison to the moving average filters. Figure 5.26 demonstrates a trade-off between accuracy near the start of combustion and pressure oscillations during combustion with the simple filters [27].

A study used five-point moving average filter for filtering the signal noise only before the start of combustion and low-pass digital filter used for another portion of engine cycle because high-amplitude pressure oscillations are produced after starting of combustion [28]. A simple moving average filter can eliminate any background system noise or random electrical noise in the cylinder pressure signal before the initiation of combustion process. The moving average filter is not able to distinguish between the bands of frequencies. The performance of moving average filter is excellent in the time domain for smoothing a measured signal. However, moving average filter performs very badly in the frequency domain for smoothing measured signal as low-pass filter [28].

The moving average filter has an extra ability to remove any five to ten point noise spike present in the cylinder pressure signal (regardless of its amplitude). The spikes are typically picked up from the interference from other devices, etc. (such as spark plug). Figure 5.27 illustrates the elimination of the abrupt background noise (spike) from the cylinder pressure signal. The filtering algorithm of moving average filter recognizes the start and end of the sudden noise spike and replaces the points with the mean value of the noise start and endpoint. The smoothing ability of the moving average filter is typically dependent on the sampling interval.

Another smoothing algorithm $(2b + 1)$ points shown by Eq. (5.14) is proposed in [29]. The smoothing equation can be applied recursively (i.e., more than once), and it shows the significant removal of noise errors.

$$a_n = \frac{1}{b^2}\left[a_{n-(b-1)} + 2a_{n-(b-2)} + 3a_{n-(b-3)} + \cdots + ba_n + \cdots + 3a_{n+(b-3)} + 2a_{n+(b-2)} + a_{n+(b-1)}\right] \tag{5.14}$$

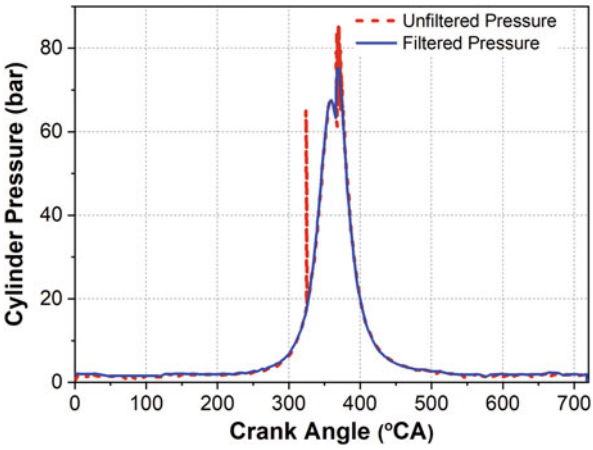

Fig. 5.27 Random noise spike filtering using moving average filter from cylinder pressure signal (Adapted from [28])

Least-square polynomial approximation (LPA) over a set of points can also be used for smoothing the cylinder pressure trace. Polynomials are the approximating functions of choice when a smooth function is to be approximated locally. However, if a function is to be approximated on a larger interval, the degree of the approximation polynomial can be unacceptably large. To solve this issue, the interval of approximation is subdivided into sufficiently small intervals in such a way that a polynomial of relatively low degree can offer a good approximation to the function interval. This polynomial approximation is performed such that the polynomial pieces blend smoothly and such smooth piecewise polynomial function is called a spline. The spline function is found to be very effective for smoothing both steady and transient cylinder pressure traces [24]. The spline function applied in the study is the cubic smoothing spline. The starting smoothing point has a significant effect on the accuracy for analyzing heat release rate and to eliminate systematic error.

Designing of filter for the combustion pressure signal faced several challenges to meet the requirement of signal processing over a wide range of operating condition (normal and abnormal). Typically, all filters introduce phase shift to a certain amount in the filtered output signal. A simple zero-phase (phase-less) filter is not an optimal smoothing method to this particular signal of combustion pressure, where a rapid increase in the signal occurs after the initiation of combustion. Even using a zero-phase digital filter for smoothing cylinder pressure signal leads to shift in the signal, and it is not able to track the abrupt pressure trace. Figure 5.28 illustrates the phase shift by zero-phase filter in the cylinder pressure signal and its comparison with five-point moving average filter. The zero-phase Butterworth filter applied to an oscillatory pressure signal is able to reduce the pressure oscillation but also adds the shift in the signal near the combustion starting point.

Identification of crucial filter parameters such as cutoff frequency, filter order, passband characteristics, etc. is an important issue particularly when the filter is applied online. Variation in engine operating conditions (speed and load) changes

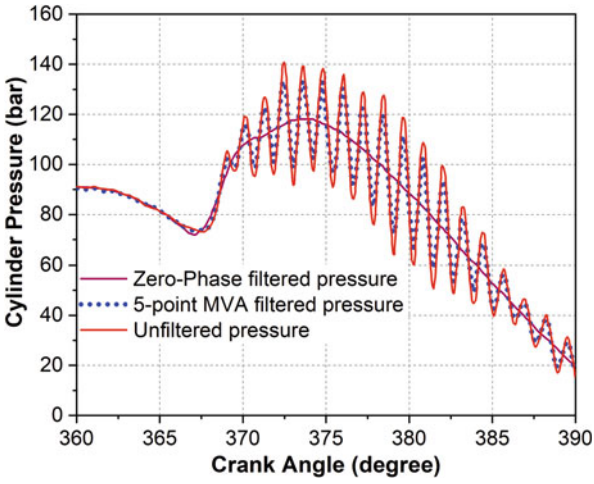

Fig. 5.28 Illustration of phase shift in filtered pressure signal with zero-phase Butterworth filter in pressure signal (Adapted from [28])

the frequency spectrum of the pressure curve. Thus, the predetermined/predefined cutoff frequency for all the engine operating condition is not a good strategy. Therefore, an adaptive method is a more suitable strategy for choosing the cutoff frequency for the cylinder pressure signal filter (particularly for online application) [28].

5.4.2 *Low-Pass FIR Filter*

Two types of digital filters are used for filtering signal noise from acquired cylinder pressure data: finite impulse response (FIR) and infinite impulse response (IIR). The impulse response (or response to any finite length input) of an FIR filter has finite duration, i.e., it settles down to zero in the finite amount of time. The phase shift in FIR filter is linear because it does not use feedback, and thus, it depends only on the input. Linear phase characteristics of FIR filter are their most significant advantage, but it needs more computation capacity in comparison to an IIR filter. The FIR filters are stable in comparison to IIR filters [28].

Payri et al. [1] developed low-pass FIR filters for offline and online filtering of the experimental cylinder pressure signal. Identification of the optimum cutoff frequency is the major problem with low-pass filter [1, 30]. The noise-to-signal ratio becomes important above the cutoff frequency. Additionally, the direct removal of the high-frequency band can lead to overshooting of the pressure signal (the Gibbs effect) which results in significant error in the heat release computation. This can be eliminated by smoothing the transition with a Hanning window [30, 31], which is defined between two cutoff frequencies: the stopband initial frequency and the stopband final frequency.

The offline FIR filter proposed is presented by Eq. (5.15) [1]:

$$P_k^{\text{filt}} = P_k \cdot \theta_k \tag{5.15}$$

$$\theta_k = \begin{cases} 1 & \text{if } k < k_c - \dfrac{k_{\text{stop}}}{2} \\ \dfrac{1}{2} \cdot \left[\cos\left(\dfrac{k - \left(k_c - \dfrac{k_{\text{stop}}}{2} \right)}{k_{\text{stop}}} \cdot \pi \right) + 1 \right] & \text{if } k_c - \dfrac{k_{\text{stop}}}{2} < k < k_c + \dfrac{k_{\text{stop}}}{2} \\ 0 & \text{if } k < k_c + \dfrac{k_{\text{stop}}}{2} \end{cases} \tag{5.16}$$

where P_k is the content of the averaged pressure signal at harmonic k and P_k^{filt} is the filtered value of the spectrum, k_c is cutoff harmonic, and k_{stop} is stopband edge harmonic. To get the averaged and filtered pressure in the temporal domain, inverse

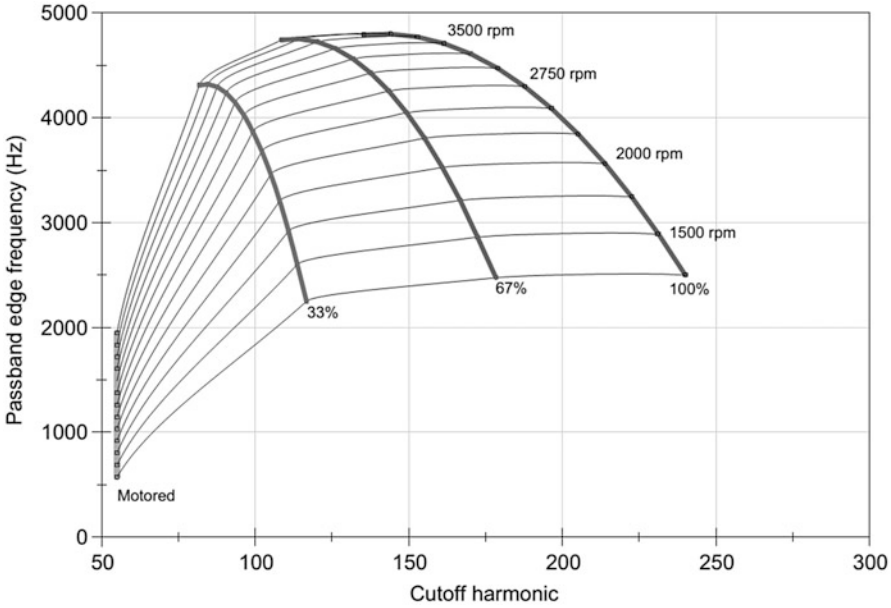

Fig. 5.29 Cutoff frequency map [1]

discrete Fourier transform (DFT) is used. The cutoff harmonic is estimated as the point where the average cycle harmonics meets with the noncyclic harmonics, attributable to signal noise and cycle-to-cycle variations.

The DFT-based filter calculation is quite a time-consuming, and acquiring several cycles before processing causes a significant delay from the data acquisition. Therefore, this method is not suitable for online filtering of the measured pressure signal. An online filter is proposed, where the cutoff frequency is estimated based on a cutoff harmonic map and fixed 1 kHz stopband is used. Figure 5.29 illustrates the cutoff frequency map for the test engine. The cutoff frequency depends on engine speed and load conditions.

In another study, Payri et al. [30] proposed an adaptive method for automatic determination of cutoff frequency for smoothing the cylinder pressure. This method is based on the statistical analysis of the DFT representation of the signal: signal-to-noise ratio is identified and used for detecting the frequency where the contribution of the noise equals that of the signal. Figure 5.30 compares the heat release rate calculated using different adaptive filters (statistical and map-based) at different engine loads. The figure suggests that map-based adaptive filter has more noise in heat release curve, and thus, statistical analysis-based adaptive filter (proposed) is better method for processing cylinder pressure signal. High repeatability is shown by this method, and it is able to adapt suitably the cutoff frequencies to the pressure signal bandwidth. Hence, this method can be used for the full engine operating range, without additional manual settings requirement.

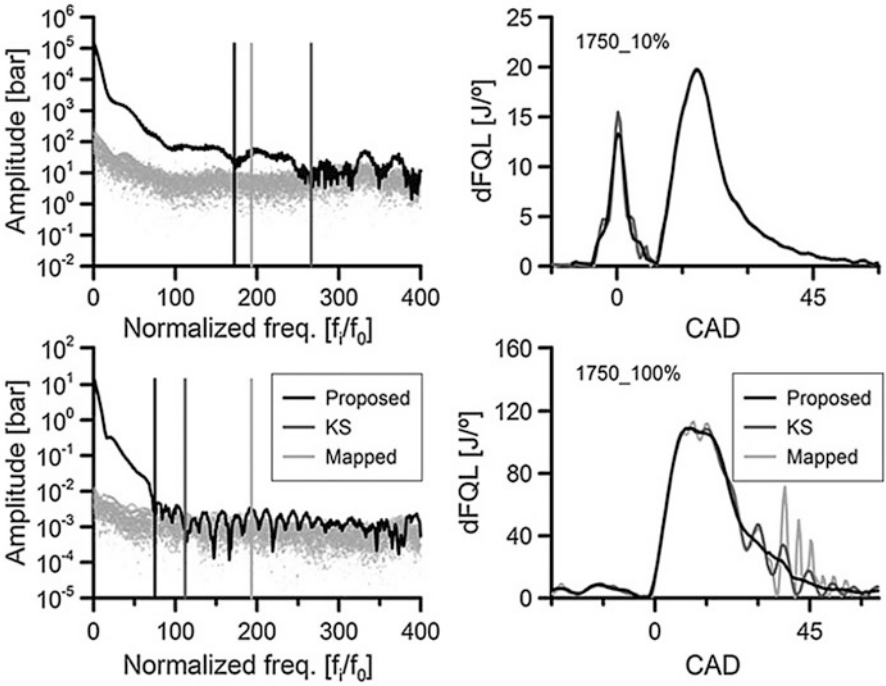

Fig. 5.30 Fourier spectra (left) and heat release rate (right) calculated using different adaptive filters at different engine loads [30]

Another study [32] proposed a procedure for designing an optimum equiripple FIR filter for filtering the combustion pressure signal of a diesel engine. A novel method of estimating the transition band frequencies and optimum filter order is presented. This method is based on discrete Fourier transform (DFT) analysis, which is the first step to determine the position of the passband and stopband frequencies. These passband and stopband frequencies are further used to estimate the most suitable FIR filter order.

5.4.3 Low-Pass IIR (Butterworth) Filters

The infinite impulse response (IIR) filter has an impulse response function, which is non-zero over an infinite length of time. The IIR filters use feedback, and thus, the phase shift is a nonlinear function of frequency. An IIR filter is also known as a recursive digital filter because its output is a function of previous outputs as well as the input. If $x[n]$ represents the nth input to the filter and $y[n]$ is the nth output of the filter, then a general IIR filter is implemented as Eq. (5.17):

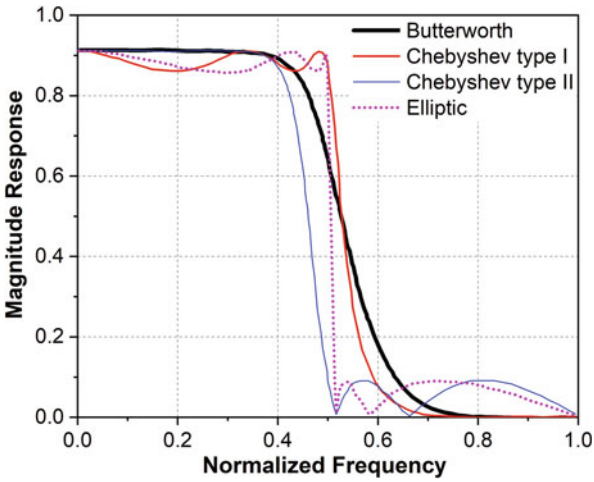

Fig. 5.31 Frequency responses of fifth-order low-pass IIR filters (Adapted from [28])

$$y[n] = a_0{}^* x[n] + a_1 x[n-1] + \cdots + a_M x[n-M] - (b_1 y[n-1] + b_2 y[n-2] + \cdots + b_N y[n-N]) \quad (5.17)$$

Equation (5.17) depicts that the nth output is a linear function of the nth input, the previous M inputs, and the previous N outputs. The coefficients "a" and "b" are computed to give the IIR filter a specific frequency response and depending on the type of filter the number of coefficients, M and N vary. The IIR filters have sharper roll-off in comparison to FIR filters of the same order, and IIR filters demand lower computation capacity in comparison to FIR filters [28].

Several type of IIR filters are available such as Chebyshev filter, Elliptic filter, Butterworth filter, Bessel filter, etc. Figure 5.31 shows the frequency responses of 5th-order low-pass IIR filters with a cutoff frequency of 0.5 normalized units. The order of the filter determines the transition from passband to stopband. Among all these filters, the Butterworth filter has the flattest passband response and poor roll-off rate. Roll-off is defined as the steepness of a response function with frequency in the transition between a passband and a stopband. Chebyshev filter has a sharper roll-off and more passband ripple (Type 1) or stopband ripple (Type 2) in comparison to a Butterworth filter. The error between the idealized and the actual filter characteristics is minimized by Chebyshev filters over the range of the filter, but filtered signal has inherent passband ripples [28]. A study [27] conducted on aviation diesel engine, showed that the Butterworth filter calculates filtered pressure with reasonable accuracy for normal combustion. However, in the case of an abnormal (erratic) combustion, the Butterworth filter leads to biases, particularly at the start of combustion with a high-pressure rise rate. The Chebyshev Type 1 filter performed well, filtering both normal and erratic combustion in-cylinder pressure data. The Chebyshev Type 1 filter with optimal parameters (fifth-order polynomial and 0.001% allowed ripples) was found to be an optimal filter for analysis of an aviation diesel engine in-cylinder data [27].

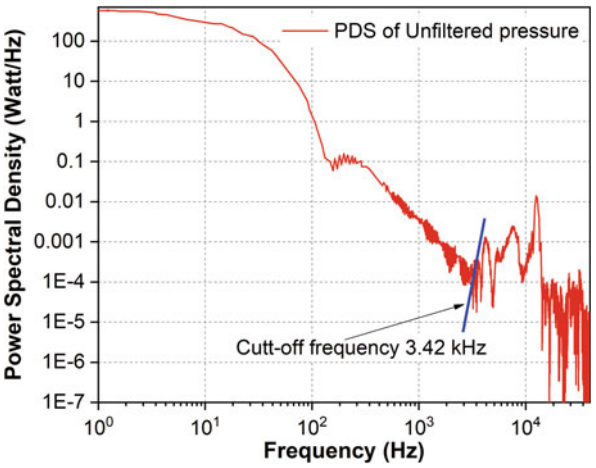

Fig. 5.32 Power spectral density for a typical cylinder pressure cycle (Adapted from [28])

Low-pass filters are suitable for removing high-frequency noise. However determination of cutoff frequency to discriminate signal and noise is the key issue. The adaptive estimation of cutoff frequencies is required for filtering the in-cylinder pressure signal because it significantly varies with engine operating conditions. A study proposed the adaptive determination of cutoff frequency by spectral analysis of cylinder pressure trace [28]. The power spectrum analysis is used to analyze the oscillations in the pressure signal in the frequency domain. Figure 5.32 shows the power spectrum a measured combustion pressure signal of a particular engine cycle. The frequency content in the power spectral density (PSD) curve is typically dependent on the running conditions of the engine (engine load, engine speed, boost pressure, EGR, etc.). The adaptive determination of cutoff frequency is required for online application of filters. The cutoff frequency needs to separate the actual signal component and the signal noise. For adaptive determination of cutoff frequency, the slope of the PSD curve (Fig. 6.32) is calculated on a point-by-point basis. To find a strong trend in the slope of the PSD curve, a ten-point moving average is computed. The frequency component of the cylinder pressure signal progressively loses power with increasing frequency (Fig. 6.32). An abrupt increasing trend (positive slope) in the slope on a decreasing (positive slope) PSD curve suggests that noise content of the signal begins to dominate over the combustion frequency content. Frequency corresponding to the slope change point is considered as the cutoff frequency. The cutoff frequency can vary on a cyclic basis as well as engine operating conditions.

The pressure trace can be divided into motoring, combustion only, and noise signal by a decomposition method proposed in [33]. The PSD curve of these three components shows that low-frequency content up to 200 Hz dominated by the motoring curve, where piston movement affects the pressure curve. The mid-frequency content from 200 Hz to 3.42 kHz (for pressure curve in Fig. 5.32) is dominated by the combustion-only PSD curve. The unaccounted noise is

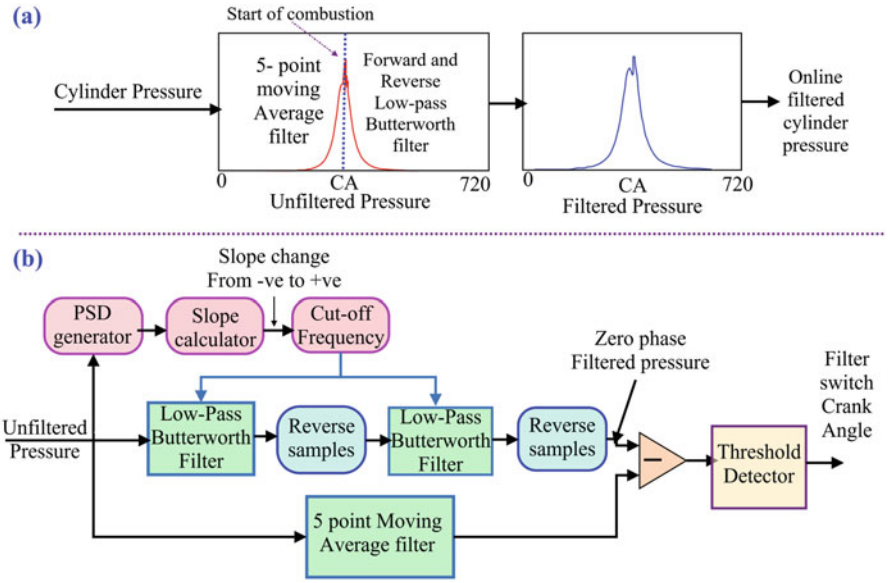

Fig. 5.33 Schematic diagram of a novel filter for cylinder pressure trace, (**a**) graphical illustration, and (**b**) flow-chart (Adapted from [28])

dominated by frequency content higher than 3.42 kHz [28]. This observation also validates the adaptive cutoff frequency determination method.

The actual information content of the cylinder pressure signal lies in frequency components in the low and mid-frequency region, and unaccounted noise is dominated in the high-frequency region. All digital filters (FIR or IIR type) lead to an inherent shift in the signal near the beginning of combustion because of an abrupt increase in the cylinder pressure signal. Therefore, a combination of two filters (five-point moving average and low-pass Butterworth filter) is used to avoid the phase shift. The schematic diagram of the proposed filter is presented in Fig. 5.33. The five-point moving average filter is applied till the start of combustion, and the Butterworth filter is used during combustion oscillations. The filter switch crank angle (start of abrupt combustion pressure) is determined by a threshold detector, which takes the difference of filtered signal of both the filters. When the difference crosses a particular threshold value, the filter switches. The cutoff frequency for the Butterworth filter is identified by the method described in Fig. 5.32. A fifth-order forward and reverse Butterworth filter (having a moderate roll-off factor) is used to filter the measured raw pressure signal. A forward and reverse Butterworth filter act as a zero-phase filter.

Figure 5.34 shows the comparison of different filter responses on the cylinder pressure signal. The five-point moving average filter works better during compression, and it is not able to remove the oscillations during combustion. The digital Butterworth filter creates a shift at the start of combustion (Fig. 6.34). However, the combined filter avoids the shift in the filtered pressure trace due to an intelligent switching between the filters just after the beginning of combustion in the cylinder.

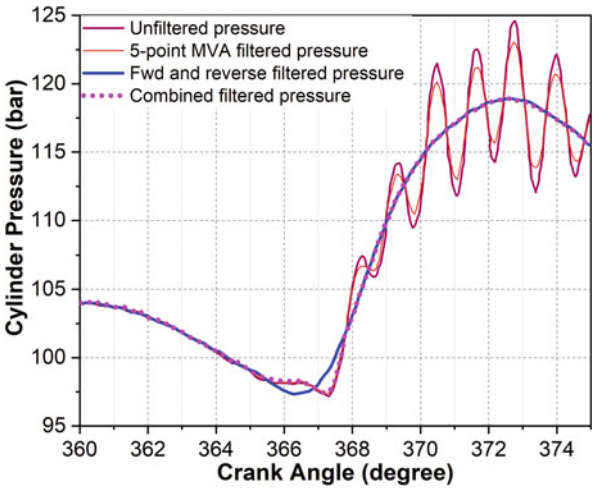

Fig. 5.34 Comparison of different filter responses on the cylinder pressure signal (Adapted from [28])

5.4.4 Thermodynamic Method-Based Filter

The measured cylinder pressure signal contains noise because of the natural characteristics of the combustion process and measurement system. Filtering/smoothing the pressure signal affects the successive heat release analysis. Several mathematical algorithms can directly smooth the cylinder pressure trace, but these methods are dependent only on mathematical algorithms. Thus, the loss of actual signal information is easier during the filtering/smoothing process. An improved methodology presented to smooth the pressure trace, which uses not only mathematic calculation but also thermodynamic knowledge [34].

In this method, average but not yet smoothed signal is used for heat release calculations. The cumulative heat release (reaction coordinate) is fitted using a series of Vibe functions. Successively, multiple Vibe functions obtained are further used as the heat release input in a single-zone simulation model to predict the pressure trace. The simulated pressure trace can be considered as a smooth characterization of the measured raw signal [34].

The combustion reaction rate (CRR) is calculated from the energy balance equation, which is presented in Eq. (5.18):

$$\mathrm{CRR} = \xi = \frac{mc_{\mathrm{v}}\left({}^{dT}/_{dt}\right) + p\left({}^{dV}/_{dt}\right) + \dot{Q}_{\mathrm{loss}}}{u_{\mathrm{comb}}} \tag{5.18}$$

The average measured pressure curve is used as the main input to the model. The Vibe combustion curve was originally proposed in [35]. The Vibe function is based

on the first principle of chain reactions, where the radical formation is proportional to the quantity of fuel in the combustion chamber and the increase of radicals is proportional to the reduction of fuel [34, 36] as represented by Eq. (5.19):

$$\frac{dm_{\mathrm{f}}^{+}}{dt} = km_{\mathrm{f}} \quad \text{and} \quad dm_{\mathrm{f}}^{+} = -\mu dm_{\mathrm{f}} \tag{5.19}$$

Then, the combustion reaction rate is calculated as Eq. (5.20):

$$\xi = \frac{dm_{\mathrm{f}}}{dt} = -\frac{k}{\mu}m_{\mathrm{f}} \tag{5.20}$$

The normalized combustion rate (Z), which is related to the normalized reaction rate (X), can be defined as Eq. (5.21):

$$z = \frac{dX}{d\tau} = \xi\frac{t_{\mathrm{comb}}}{m_{\mathrm{f},0}} \quad \text{and} \quad \mathrm{X} = \frac{m_{\mathrm{f}}}{m_{\mathrm{f},0}} \tag{5.21}$$

where τ is normalized time ($\tau = t/t_{\mathrm{comb}}$). Vibe proposed a model assuming a nonlinear time dependency of the reaction constant ($k \propto t^{m}$). The normalized reaction rate and reaction coordinate can be represented as Eq. (5.22):

$$Z = a(m+1)\tau^{m}\mathrm{e}^{-a\tau^{m+1}} \quad \text{and} \quad X = 1 - \mathrm{e}^{-a\tau^{m+1}} \tag{5.22}$$

A series progression of Vibe functions was proposed for heat release calculation [37] as presented in Eq. (5.23):

$$X = \sum_{k=1}^{n} b_k X_k = \sum_{k=1}^{n} b_k\left(1 - \mathrm{e}^{-a\tau^{m_k+1}}\right) \tag{5.23}$$

The normalized reaction rate (X) can be fitted using a nonlinear least-square fitting theory with different orders of Vibe function, assuming $m_{\mathrm{f},0}$ is known. The heat release characteristics of the cylinder are captured by fitting the parameters of multiple Vibe functions. The fitted multiple Vibe functions are used as an input for the estimation of the smoothed pressure signal using "cylinder process simulation model" [34]. It demonstrated that this method is able to remove the pressure oscillations. Additionally, three Vibe functions are the minimum, and four or five Vibe fitting functions are sufficient to get the heat release data with sufficient accuracy for that particular engine [34].

5.4.5 *Wavelet Filtering*

Computation of combustion metrics without careful noise rejection techniques affects the feedback control by bringing inaccurate or time-delayed signals to the feedback control system. A study developed a technique for de-noising pressure signals for the same cycle feedback control using a wavelet filter [38]. Wavelet filters allowed tuning of de-noising characteristics as a function of sampling crank angle resolution and desired noise elimination capability.

The wavelet-based method is known for effectively removing noise from a signal by identifying which component or components (of the signal) contain the noise and then reconstructing the signal without those parasitic components [39]. The wavelet de-noising process involves down-sampling of the convoluted signal, which in general leads to signal aliasing except when the convolution process involves a wavelet acting as a transfer function [38]. The convolution of the pressure signal with a transfer function is a desirable filtering option because the pressure signal being filtered consists of a fixed number of samples in an array consisting of a predefined positioning of the samples on the angular scale. To facilitate efficient filtration of noise affected pressure signals, wavelets are considered as the transfer function. The wavelet filter does not cause lag in signals, allowing for accurate estimation of the signal mean in the presence of noise without distorting the signal response with respect to crank angle. Wavelet-based filtration are fully immune to engine speed changes as the shape of the signal does not change with the engine speed and wavelets respond only to the pattern of sampling (number and distance between samples) [38].

5.5 Cycle Averaging of Measured Data

For automotive engine research and development, the cylinder pressure signal is always an important experimental diagnostic parameter, and it can provide the large amount of information by correct processing such as combustion phasing, thermal efficiency, knocking, cyclic torque variability, intake and exhaust tuning, cylinder balance, structural loading, and cyclic fueling variability [40]. Measured cylinder pressure data is also used for validation of various engine combustion models. For these purposes, typically ensemble averaged cylinder pressure (as a function of crank angle) is used to get the mean at desired accuracy, which further used to find average performance and combustion parameters. Thus, the averaged cylinder pressure must be robust to cycle-to-cycle variations in the signal. Additionally, mean average variables (fuel mass flow, air mass flow, engine speed, etc.) are used generally for an accurate heat release rate estimation. Therefore, it is important to average the measured cylinder pressure signals so that a representative (close to actual) thermodynamic cycle can be analyzed [1].

The cylinder pressure signal is typically oscillating and varying on cycle-to-cycle basis. The oscillation in the cylinder pressure signal can be partly due to the combustion process. Both chemical and physical phenomena are responsible for cycle-to-cycle variations. Various factors can be considered for combustion variations such as the variations in the fuel-air ratio, the residual gas fraction, the fuel composition, and the motion of unburned gas in the combustion chamber [40]. Cyclic variations can easily be recognized by plotting a number of engine cycle pressure data on one figure (Fig. 5.23). The stochastic (random) fluctuations in pressure signal can be removed by averaging the number of cycles. However, the systematic errors cannot be eliminated by averaging. Other important factors for pressure signal fluctuations are signal conversion, signal transmission, analog-to-digital conversion, etc.

Numerous consecutive engine pressure cycles are typically measured to minimize the cyclic variations. Any randomly selected engine combustion cycle may not be representative of the steady-state operation of the engine. The optimal number of cycles to be averaged for representing a steady-state operation of the engine depends on the type of engine combustion mode, the data acquisition system, and the engine operating conditions [1, 41, 42]. Generally, the engine stability is the major issue in the determination the number of cycles to be considered for averaging. In diesel engines, a lower number of cycles are typically required because of its relatively lower cyclic variation in comparison to corresponding spark ignition engine. The thermo-fluid dynamic processes are more stable in a diesel engine. Even for the same engine, different engine operating conditions have different levels of cyclic variations due to engine stability [1]. Typically, engines are more steady and stable at higher speed and load conditions, and lower load conditions (particularly idle operating conditions) have higher variations. Cylinder pressure data acquisition system can also affect the optimal number of cycle to record, in addition to the engine and operating point stability [22]. Additionally, the number of cycles to be recorded also depends on the most critical or demanding application for which data is recorded [43]. The optimal number of cycles to analyze the pressure rise rate or the heat release rate is not necessarily the same [2].

In most of the published study, experience-based rules are mostly used depending on the application. Two statistical methods are discussed for determination of optimal cycle number in the following subsections.

5.5.1 Method Based on Standard Deviation Variations

In this method, the variations in the standard deviation of the measured data at each crank angle position are used to determine the optimal number of cycle to measure. The optimal number of cycles is considered as the number of cycles where a further increase in the number of cycles will not improve the precision of the estimated results. To estimate the optimal number of cycles, the first large number of cycles (M) of pressure data is recorded using the high-speed data acquisition system. Next,

a set of mean engine cycle (j) is calculated for a different number of selected cycles (m) using the Eq. (5.24):

$$\bar{Y}_{m,j}(\theta) = \frac{1}{m}\sum_{i=j}^{j+m} Y_i(\theta) \tag{5.24}$$

where Y_i is a particular signal during ith cycle and θ is the crank angle (CA) position. Y_i can be a pressure or pressure rise rate or heat release rate signal. For every selected number of cycles, a set of $M - m + 1$ average signal $Y_{m,j}$ can be determined. The standard deviation as a function of crank angle position is calculated using Eq. (5.25) for each set:

$$\sigma_m(\theta) = \sigma_m\{Y_{m,j}(\theta)\} \tag{5.25}$$

There exists a variation of standard deviation in all set ($M - m + 1$) at every crank angle position, and using a range of variation in standard deviation at each position, a maximum and a minimum envelope curve can be derived. Figure 5.35 presents the variations of the standard deviation (for $m = 5$) as a function of crank angle position for the cylinder pressure traces recorded for 3000 consecutive engine cycles in HCCI engine. There is a 2996 set of data can be derived when five cycles are selected for 3000 consecutive engine cycles recorded. At each crank angle position, 2996 values of standard deviation are computed, and one such variation is shown with the thin

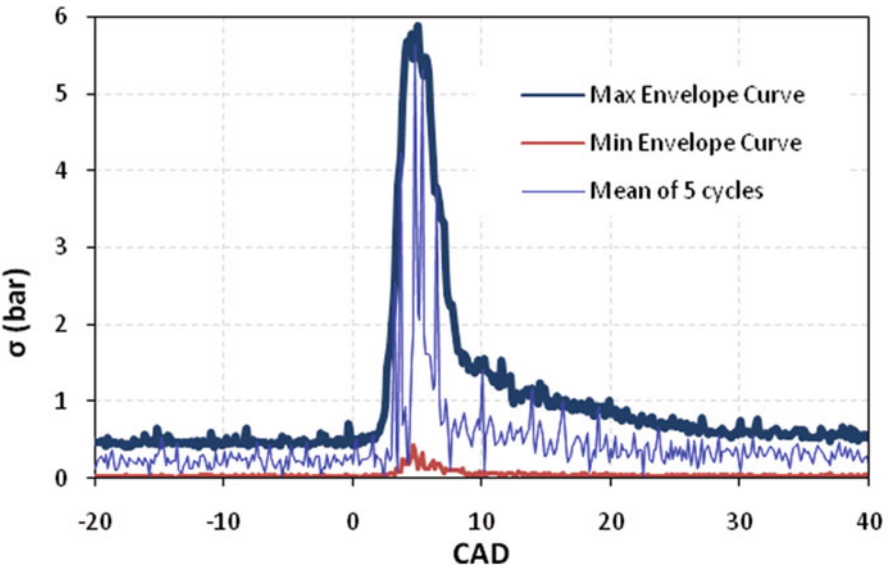

Fig. 5.35 Standard deviation and its maximum and minimum envelope curves of five averaged pressure cycles in HCCI engine [2]

blue line (Fig. 5.35). The upper and lower bold lines in Fig. 5.35 correspond to the maximum and minimum value of standard deviation at each crank angle position. The figure clearly shows that the variations in the standard deviation of the pressure signal are dependent on the crank angle position, and it is higher during the combustion period. The large increase in the standard deviation is because of higher cyclic variations in the combustion process.

Figure 5.36 shows the variations in standard deviation as a function of crank angle position with different number of cycles selected for averaging for cylinder pressure signal (with and without filter) in HCCI engine. The maximum and minimum envelope curve (as derived in Fig. 5.35) is presented with a different color for different numbers of cycles. Standard deviation value decreases with higher in number of cycles selected, and this trend is the same for both filter and non-filter pressure trace. The higher value of the standard deviation is lower for filtered pressure trace (Fig. 5.36b). The area between the maximum and minimum envelope curve also shrinks with the increasing number of cycles for both without filter and filtered pressure trace.

The maximum difference between the maximum and minimum standard deviation curves $\{(\sigma_{\max} - \sigma_{\min})_{\max}\}$ in whole engine cycle is calculated for all the test conditions without filter and with different filters. Figure 5.37 presents the variations of $(\sigma_{\max} - \sigma_{\min})_{\max}$ with different numbers of cycles selected for averaging at different HCCI engine operating conditions for pressure signal without filter and with different filters. The values of $(\sigma_{\max} - \sigma_{\min})_{\max}$ are higher for raw pressure signal (without filter) in comparison to filtered pressure signal. The figure also depicts that the $(\sigma_{\max} - \sigma_{\min})_{\max}$ value decreases rapidly with higher number of selected cycles. The value of $(\sigma_{\max} - \sigma_{\min})_{\max}$ does not reduce after particular number for selected cycles in all the four cases, which means adding further number of cycles will not decrease the standard deviation and also will not improve the precision of the mean value. This observation suggests that this is the optimal point of number of cycles and the additional cycle will not increase the accuracy of results too much. Figure 5.37 also depicts that the minimum number of cycles (the point where additional cycle has no improvement in standard deviation) is highly dependent on engine operating condition and the type of filter used to smooth the pressure data. Single optimal number of cycles for all the operating conditions can be determined on the basis of the allowed threshold value of $(\sigma_{\max} - \sigma_{\min})_{\max}$. Value of number of cycles at which $(\sigma_{\max} - \sigma_{\min})_{\max}$ values are less than a threshold value can be considered as the optimal required number of cycles for analysis [2, 41]. The similar analysis is also conducted for calculated pressure rise rate and heat release rate; the optimal number of cycles is different depending on the application. A more complete detail can be found in the original study [2].

The value of $(\sigma_{\max} - \sigma_{\min})_{\max}$ also depends on the engine combustion mode. Figure 5.38 shows the variations of $(\sigma_{\max} - \sigma_{\min})_{\max}$ with different number of cycles selected for averaging cylinder pressure trace in a diesel engine. It can be noticed that for this particular operating condition, the optimal number of cycle is 25, which is very less in comparison to the HCCI engine (Fig. 5.37).

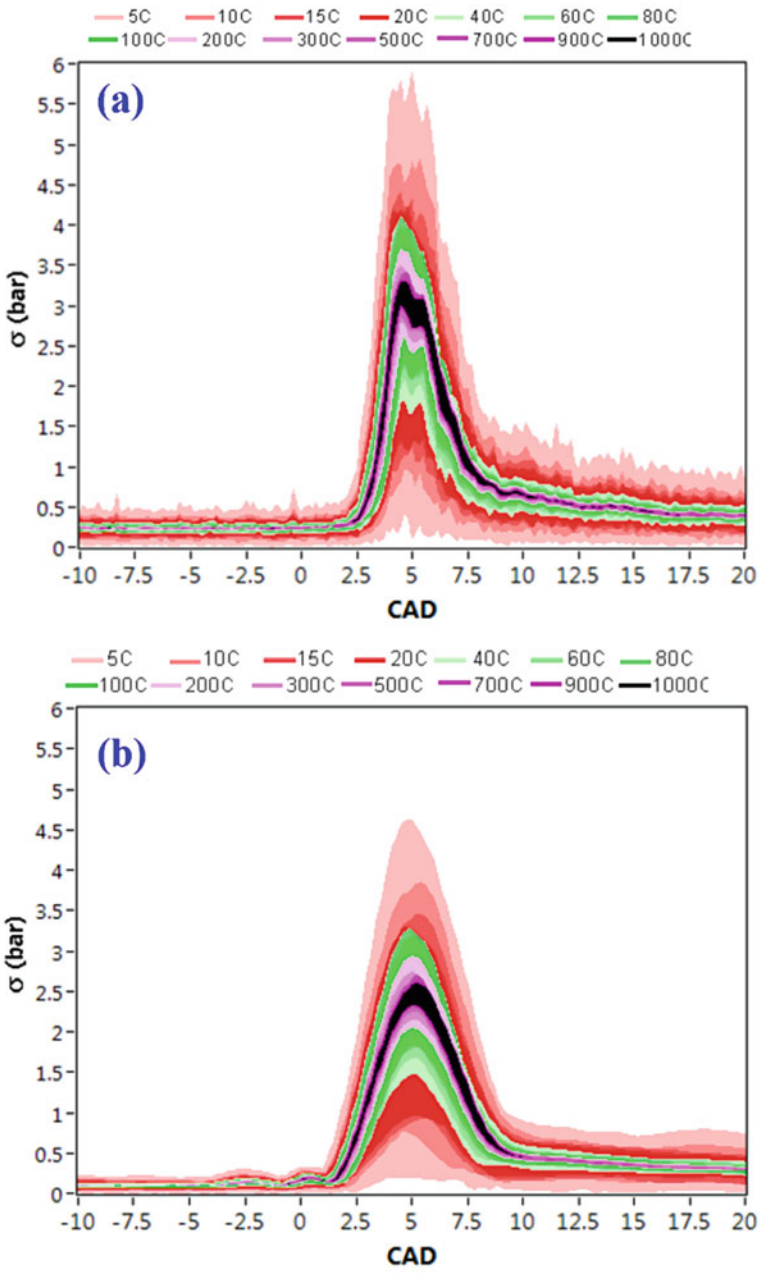

Fig. 5.36 Variations in standard deviation with different number of cycles selected for averaging for cylinder pressure in HCCI engine at 1200 rpm and $\lambda = 2.1$. (**a**) No filter. (**b**) Savitzky-Golay filter [2]

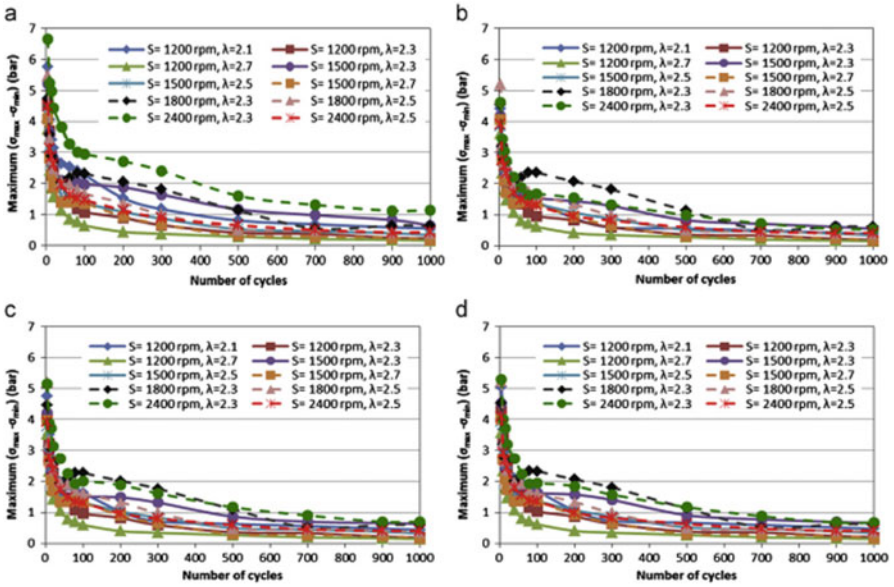

Fig. 5.37 Variation of the $(\sigma_{max} - \sigma_{min})_{max}$ with different number of cycles selected for averaging the pressure signal at different operating conditions of HCCI engine. (**a**) No filter, (**b**) Savitzky-Golay filter, (**c**) zero-phase filter, and (**d**) Butterworth filter [2]

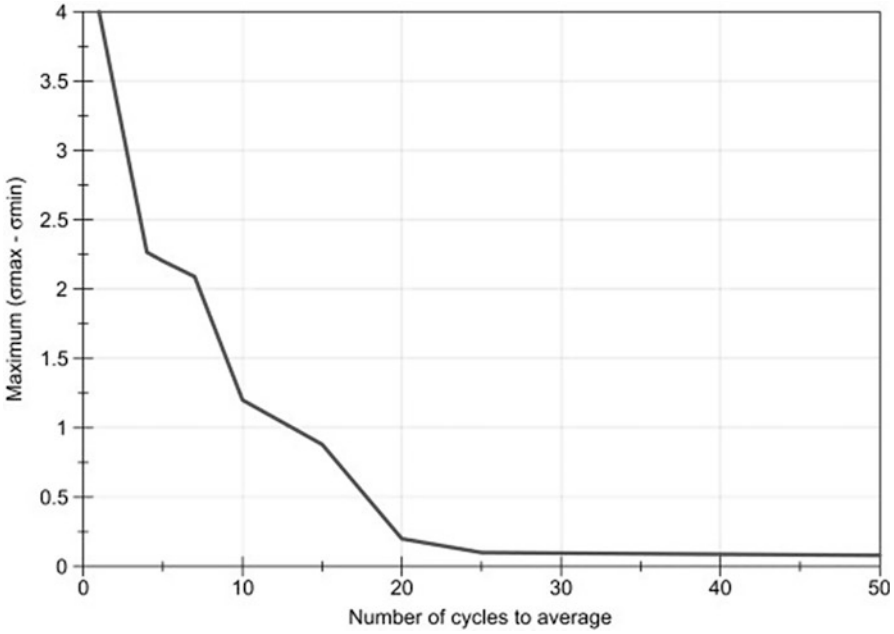

Fig. 5.38 Evolution of the $(\sigma_{max} - \sigma_{min})_{max}$ with different the number of cycles selected for averaging cylinder pressure in a diesel engine [1]

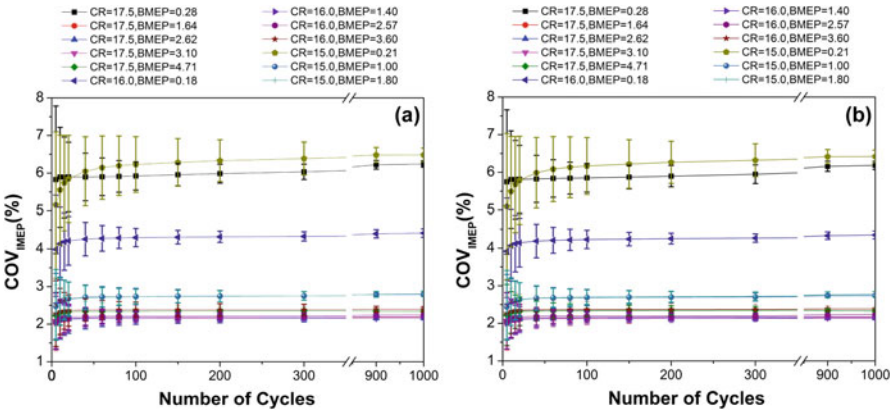

Fig. 5.39 The variation of COV_{IMEP} with different number of cycles in a convention diesel engine for (**a**) no filter and (**b**) Butterworth filter [41]

To estimate the indicated engine performance, typically indicated mean effective pressure (IMEP) is used. Noise in the cylinder pressure signal and cycle-to-cycle variation in pressure signal result in the significant variation in IMEP value. The coefficient of variation (COV) of IMEP is typically used to characterize engine stability at particular engine operating point. To determine the optimum number of cycles for lower variation in the IMEP calculation, the COV_{IMEP} is evaluated at various operating conditions for different number of cycles using the data of 2500 consecutive cycles (Fig. 5.39). For each number of cycles selected for calculation, the variation of COV_{IMEP} is determined, the average value is shown by symbol, and the standard deviation is represented as error bars (Fig. 5.39). The figure depicts that average values and standard deviation of COV_{IMEP} reduces with higher engine load. The variation of IMEP is also higher at lower compression ratio (CR). Figure 5.39 also illustrates that filtering the pressure trace does not lead to a significant reduction in standard deviation of COV_{IMEP} (error bars). To eliminate the cyclic variations, the number of cycles that can be used depends on engine operating conditions. For standard deviation of COV_{IMEP} less than 0.5, lower numbers of cycles (up to 60 cycles) are needed at higher engine load conditions in comparison to idle conditions (up to 200 cycles) [41].

5.5.2 Method Based on Statistical Levene's Test

In this method, the optimal number of cycles is determined using statistical Levene's test. After recording the sufficient number for pressure cycles, the data is divided into bundles of first 10, 20, 30, and so on and number of engine cycles. The standard deviation of IMEP (σ_{IMEP}) data in all the groups is calculated. In order to determine the optimal number of cycles, it is essential to show that the additional data after a

certain point do not significantly vary the statistics of σ_{IMEP}. It means there is no need for an additional number of cycles for achieving a correct value of COV_{IMEP} if standard deviation remains the same as with the increase in cycle number [40].

The Levene's test is used because it provides better results under non-normality conditions [44], and the IMEP data may not be necessarily normally distributed. In this test, the test value M calculated by Eq. (5.26) is usually compared with the critical value of F-distribution for the particular degree of freedom and significance level (p-value). The null hypothesis that is "variances of the groups are equal" is rejected if the p-value is lower than the determined significance level (usually 0.05) otherwise accepted. The p-value calculated by Eq. (5.27) and is defined as the probability that a randomly drawn number from the F-distribution is greater than or equal to the test value achieved. Thus, the p-value depicts how strong evidence is for null hypothesis. The higher the p-value provides, the stronger evidence for the null hypothesis to be true [45]. This suggests that there is no requirement of an additional number of cycles to obtain true variance value if the p-value is large enough [40]. Therefore, the cycle number at which variance continuously remains constant afterward can be an optimal number of cycle. A more complete detail can be found in the original study [40]:

$$M = \frac{(N-k)\sum_{i=1}^{k} N_i \left(\bar{Z}_{i.} - \bar{Z}_{i..}\right)^2}{(k-1)\sum_{i=1}^{k}\sum_{j=1}^{N_i}\left(\bar{Z}_{ij} - \bar{Z}_{i.}\right)^2} \tag{5.26}$$

where $Z_{i.}$ is group mean and $Z_{i..}$ is overall mean, $Z_{ij} = \left|\text{Y}_{\text{ij}} - \mathbf{Y_{i.}}\right|$, Y_{ij} is i^{th} data of j^{th} group, and $\mathbf{Y_{i.}}$ is mean of the i^{th} group.

$$P\text{-value} = p\left(M \le F_{v1;v2}\right) \text{ is the probability that } M \text{ is smaller than } F_{v1;v2} \tag{5.27}$$

Figure 5.40 presents the variations of p-values with the relative air-fuel ratio and engine operating speed with different number of selected cycles. The p-value reaches near the value 1 for 50 cycles for both engine operating conditions (Fig. 5.40). After 50 engine cycles, the p-value remains high between 0.9 and 1 value which is the important factor for the null hypothesis test. Thus, it is concluded that 50 cycles are enough to estimate the true covariance value and to achieve the average pressure cycle at various engine operating conditions.

Discussion/Investigation Questions

1. Differentiate between static and dynamic TDC determination methods, and discuss their merits and demerits.
2. Why two points of measurement at sufficiently away from TDC is selected during static TDC determination using dial gauge instead of taking the measurement exactly at TDC position? What is the optimum position for dial gauge measurement for static TDC determination? Justify your answer.

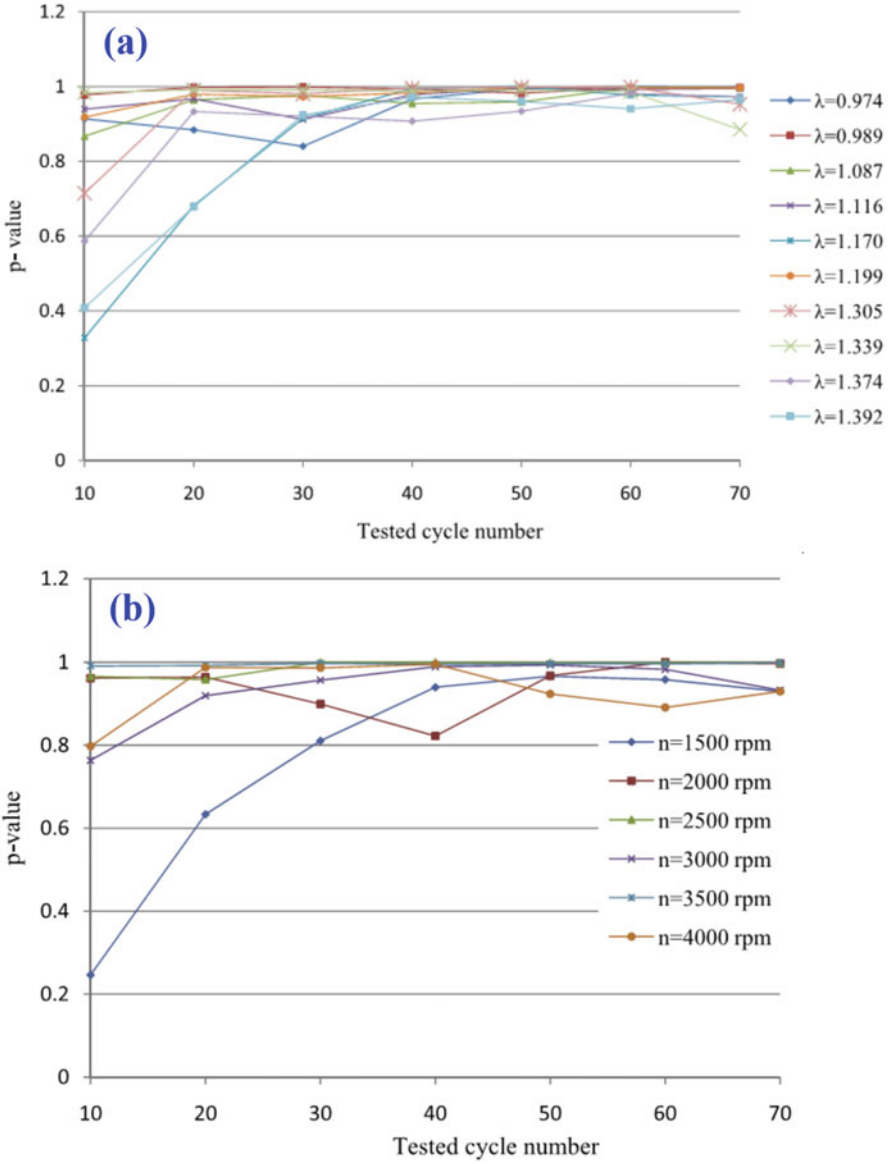

Fig. 5.40 The *p*-value variations with different cycle numbers at different (**a**) air-fuel ratios and (**b**) engine speeds [40]

3. Discuss the working principle of capacitive TDC sensor used for dynamic determination of TDC position. Write the advantages and disadvantages of TDC estimation using this method.

4. Draw typical output signal from capacitive TDC sensor for whole engine cycle of the four-stroke engine. Discuss the method for determination of compression TDC and gas exchange TDC positions.
5. Discuss the effect of the shape of the piston's upper surface on TDC sensor mounting and its signal output.
6. What is the thermodynamic loss angle? Explain the factors affecting the thermodynamic loss angle. Discuss the dependency of thermodynamic loss angle with engine speed.
7. Explain two thermodynamic methodologies of TDC determination in IC engines based on a motoring in-cylinder pressure data.
8. Make a list of the important combustion parameters affected by absolute pressure referencing error, and discuss whether the referencing error is affected by engine operating load. Write a performance or combustion parameter which is not affected by absolute pressure referencing, and justify your answer.
9. Why accurate pressure referencing is essential for mean and individual engine combustion cycle when combustion pressure is measured using a quartz piezoelectric transducer?
10. Discuss the different (at least three) methods used for pegging in-cylinder pressure data. How will you choose the pegging method for noisy in-cylinder pressure data? Discuss the possible error introduced in the cylinder pressure data due to pegging method and how these errors can be eliminated?
11. Discuss the best crank angle position for absolute pressure referencing using inlet and outlet manifold pressure sensor. Comment on the characteristics of pressure sensors required for both intake and exhaust manifold.
12. Discuss the limitations of absolute pressure referencing using intake or exhaust manifold pressure sensor.
13. Explain an efficient method of pegging calculation for real-time in-cylinder pressure offset compensation. Discuss why onboard cylinder pressure signal analysis is important.
14. Discuss the reasons for the higher preference for the polytropic exponent method for pressure correction over the manifold pressure referencing. Discuss the demerits of cylinder pressure correction using the polytropic exponent method.
15. Why filtering of in-cylinder pressure signal is required? Discuss the different methods of filtering/smoothening of the cylinder pressure signal. How optimal filtering frequency can be calculated for a given cylinder pressure signal?
16. Explain a method for adaptive determination of cutoff frequencies for filtering the cylinder pressure signal.
17. What are the sources of noise in the cylinder pressure signal of internal combustion engines? Discuss the different ways to remove the signal noise from the measured cylinder pressure signal by a piezoelectric pressure signal.
18. Differentiate between two types of digital filters, i.e., finite impulse response (FIR) and infinite impulse response (IIR), applied for filtering noise from measured cylinder pressure data.

19. Why averaging of cylinder pressure is done over a different number of cycles? Discuss the case when averaging cannot be done over cycles. Discuss a method for deciding the number of cycles sufficient for averaging.
20. Discuss the typical number of cycles that can be used in averaging for heat release analysis in CI, SI, and HCCI engines. Justify your answer based on the combustion process in three modes of engine combustion.

References

1. Payri, F., Luján, J. M., Martín, J., & Abbad, A. (2010). Digital signal processing of in-cylinder pressure for combustion diagnosis of internal combustion engines. *Mechanical Systems and Signal Processing, 24*(6), 1767–1784.
2. Maurya, R. K., Pal, D. D., & Agarwal, A. K. (2013). Digital signal processing of cylinder pressure data for combustion diagnostics of HCCI engine. *Mechanical Systems and Signal Processing, 36*(1), 95–109.
3. Luján, J. M., Bermúdez, V., Guardiola, C., & Abbad, A. (2010). A methodology for combustion detection in diesel engines through in-cylinder pressure derivative signal. *Mechanical Systems and Signal Processing, 24*(7), 2261–2275.
4. Rogers, D. R. (2010). *Engine combustion: Pressure measurement and analysis*. Warrendale: Society of Automotive Engineers.
5. Tazerout, M., Le Corre, O., & Rousseau, S. T. D. C. (1999). *TDC determination in IC engines based on the thermodynamic analysis of the temperature-entropy diagram* (No. 1999-01-1489). SAE Technical Paper.
6. Žvar Baškovič, U., Vihar, R., Mele, I., & Katrašnik, T. (2017). A new method for simultaneous determination of the TDC offset and the pressure offset in fired cylinders of an internal combustion engine. *Energies, 10*(1), 143.
7. Pischinger, R. (2002). *Engine indicating user handbook*. Graz: AVL List GmbH.
8. Bueno, A. V., Velásquez, J. A., & Milanez, L. F. (2012). Internal combustion engine indicating measurements. In Md. Z. Haq (Eds.), *Applied measurement systems*. InTech.
9. Yamanaka, T., & Kinoshita, M. (1991). Optimum probe design for precise TDC measurement using a microwave technique. *Journal of Engineering for Gas Turbines and Power, 113*(3), 406–412.
10. Yamanaka, T., Esaki, M. I. C. H. I. R. U., & Kinoshita, M. A. S. A. O. (1985). Measurement of TDC in engine by microwave technique. *IEEE Transactions on Microwave Theory and Techniques, 33*(12), 1489–1494.
11. REVelation operator reference manual. (2004). Madison: Hi-Techniques.
12. Maurya, R. K. (2018). *Characteristics and control of low temperature combustion engines: Employing gasoline, ethanol and methanol*. Cham: Springer.
13. Brunt, M. F., & Pond, C. R. (1997). *Evaluation of techniques for absolute cylinder pressure correction* (No. 970036). SAE Technical Paper.
14. Sun, W., Du, W., Dai, X., Bai, X., & Wu, Z. (2017). *A cylinder pressure correction method based on calculated polytropic exponent* (No. 2017-01-2252). SAE Technical Paper.
15. Teichmann, R., Wimmer, A., Schwarz, C., & Winklhofer, E. (2012). Combustion diagnostics. In G. P. Merker, C. Schwarz, & R. Teichmann (Eds.), *Combustion engines development* (pp. 39–117). Berlin: Springer.
16. Kaul, B. C., Lawler, B. J., Finney, C. E., Edwards, M. L., & Wagner, R. M. (2014). *Effects of data quality reduction on feedback metrics for advanced combustion control* (No. 2014-01-2707). SAE Technical Paper.

17. Maurya, R. K., & Agarwal, A. K. (2013). Investigations on the effect of measurement errors on estimated combustion and performance parameters in HCCI combustion engine. *Measurement, 46*(1), 80–88.
18. Davis, R. S., & Patterson, G. J. (2006). *Cylinder pressure data quality checks and procedures to maximize data accuracy* (No. 2006-01-1346). SAE Technical Paper.
19. Lee, K., Kwon, M., Sunwoo, M., & Yoon, M. (2007). *An in-cylinder pressure referencing method based on a variable polytropic coefficient* (No. 2007-01-3535). SAE Technical Paper.
20. Lee, K., Yoon, M., & Sunwoo, M. (2008). A study on pegging methods for noisy cylinder pressure signal. *Control Engineering Practice, 16*(8), 922–929.
21. Klein, P., Schmidt, M., & Loffeld, O. (2007). Estimation of the cylinder pressure offset and polytropic exponent using extended Kalman filter. *IFAC Proceedings Volumes, 40*(10), 175–182.
22. Randolph, A. L. (1990). Methods of processing cylinder-pressure transducer signals to maximize data accuracy. *SAE Transactions,* (900170), 191–200.
23. Tunestal, P., Hedrick, J. K., & Johansson, R. (2001). Model-based estimation of cylinder pressure sensor offset using least-squares methods. In *Proceedings of the 40th IEEE Conference on Decision and Control, 2001* (Vol. 4, pp. 3740–3745).
24. Zhong, L., Henein, N. A., & Bryzik, W. (2004). *Effect of smoothing the pressure trace on the interpretation of experimental data for combustion in diesel engines* (No. 2004-01-0931). SAE Technical Paper.
25. Bueno, A. V., Velásquez, J. A., & Milanez, L. F. (2009). A new engine indicating measurement procedure for combustion heat release analysis. *Applied Thermal Engineering, 29*(8–9), 1657–1675.
26. Randolph, A. L. (1994). *Cylinder-pressure-based combustion analysis in race engines* (No. 942487). SAE Technical Paper.
27. Kim, K. S., Szedlmayer, M. T., Kruger, K. M., & Kweon, C. B. M. (2017). *Optimization of in-cylinder pressure filter for engine research* (No. ARL-TR-8034). US Army Research Laboratory Aberdeen Proving Ground United States.
28. Dey, K. (2012). *Characterization and rejection of noise from in-cylinder pressure traces in a diesel engine* (Master's Thesis). University of Windsor.
29. Stone, R. (1999). *Introduction to internal combustion engines*. London: Macmillan Press Ltd.
30. Payri, F., Olmeda, P., Guardiola, C., & Martín, J. (2011). Adaptive determination of cut-off frequencies for filtering the in-cylinder pressure in diesel engines combustion analysis. *Applied Thermal Engineering, 31*(14–15), 2869–2876.
31. Shi, S. X., & Sheng, H. Z. (1987). Numerical simulation and digital signal processing in measurements of cylinder pressure of internal combustion engines. In *Proceedings of the Institution of Mechanical Engineers International Conference on Computers in Engine Technology (C345) C20/87* (pp. 211–218).
32. Rašić, D., Baškovič, U. Ž., & Katrašnik, T. (2017). Methodology for processing pressure traces used as inputs for combustion analyses in diesel engines. *Measurement Science and Technology, 28*(5), 055002.
33. Payri, F., Broatch, A., Tormos, B., & Marant, V. (2005). New methodology for in-cylinder pressure analysis in direct injection diesel engines—Application to combustion noise. *Measurement Science and Technology, 16*(2), 540.
34. Ding, Y., Stapersma, D., Knoll, H., & Grimmelius, H. T. (2011). A new method to smooth the in-cylinder pressure signal for combustion analysis in diesel engines. *Proceedings of the Institution of Mechanical Engineers, Part A: Journal of Power and Energy, 225*(3), 309–318.
35. Vibe, I. I., & Meißner, F. (1970). *Brennverlauf und kreisprozess von verbrennungsmotoren*. Berlin: Verlag Technik.
36. Stapersma, D. (2009). *Diesel engines, volume 3: Combustion* (5th print, pp. 636–660). Den Helder: Royal Netherlands Naval College.
37. Knobbe, E., & Stapersma, D. (2001, May). Some new ideas for performing heat release analysis. In *23rd CIMAC Conference*, Hamburg, Germany.

38. Malaczynski, G. & Foster, M. (2018) *Wavelet filtering of cylinder pressure signal for improved polytropic exponents, reduced variation in heat release calculations and improved prediction of motoring pressure & temperature* (SAE Technical Paper 2018-01-1150).
39. Donoho, D. L., & Johnstone, I. M. (1995). Adapting to unknown smoothness via wavelet shrinkage. *Journal of the American Statistical Association, 90*(432), 1200–1224.
40. Ceviz, M. A., Çavuşoğlu, B., Kaya, F., & Öner, İ. V. (2011). Determination of cycle number for real in-cylinder pressure cycle analysis in internal combustion engines. *Energy, 36*(5), 2465–2472.
41. Maurya, R. K. (2016). Estimation of optimum number of cycles for combustion analysis using measured in-cylinder pressure signal in conventional CI engine. *Measurement, 94*, 19–25.
42. Brunt, M. F., & Emtage, A. L. (1996). Evaluation of IMEP routines and analysis errors. *SAE Transactions*, 105(960609), 749–763.
43. Lancaster, D. R., Krieger, R. B., & Lienesch, J. H. (1975). Measurement and analysis of engine pressure data. *SAE Transactions, 84*, 155–172.
44. Levene, H. (Ed.). (1960). *Contributions to probability and statistics: essays in honor of Harold Hotelling*. Stanford: Stanford University Press.
45. Vardeman, S. B. (1994). *Statistics for engineering problem solving*. Duxbury Press.